american physiological society

JNP JOURNAL OF NEUROPHYSIOLOGY

J Neurophysiol 129: 1191–1211, 2023.
First published March 29, 2023; doi:10.1152/jn.00302.2021

RESEARCH ARTICLE

Higher Neural Functions and Behavior

Eye movements disrupt EEG alpha-band coding of behaviorally relevant and irrelevant spatial locations held in working memory

Tom Bullock,[1,2] Kamryn Pickett,[1] Anabel Salimian,[1] Caitlin Gregory,[1,2] Mary H. MacLean,[1,2] and Barry Giesbrecht[1,2,3]

[1]*Department of Psychological and Brain Sciences, University of California, Santa Barbara, California, United States;* [2]*Institute for Collaborative Biotechnologies, University of California, Santa Barbara, California, United States; and* [3]*Interdepartmental Graduate Program in Dynamical Neuroscience, University of California, Santa Barbara, California, United States*

Abstract

Oscillations in the alpha frequency band (~8–12 Hz) of the human electroencephalogram play an important role in supporting selective attention to visual items and maintaining their spatial locations in working memory (WM). Recent findings suggest that spatial information maintained in alpha is modulated by interruptions to continuous visual input, such that attention shifts, eye closure, and backward masking of the encoded item cause reconstructed representations of remembered locations to become degraded. Here, we investigated how another common visual disruption—eye movements—modulates reconstructions of behaviorally relevant and irrelevant item locations held in WM. Participants completed a delayed estimation task, where they encoded and recalled either the location or color of an object after a brief retention period. During retention, participants either fixated at the center or executed a sequence of eye movements. Electroencephalography (EEG) was recorded at the scalp and eye position was monitored with an eye tracker. Inverted encoding modeling (IEM) was applied to reconstruct location-selective responses across multiple frequency bands during encoding and retention. Location-selective responses were successfully reconstructed from alpha activity during retention where participants fixated at the center, but these reconstructions were disrupted during eye movements. Recall performance decreased during eye-movements conditions but remained largely intact, and further analyses revealed that under specific task conditions, it was possible to reconstruct retained location information from lower frequency bands (1–4 Hz) during eye movements. These results suggest that eye movements disrupt maintained spatial information in alpha in a manner consistent with other acute interruptions to continuous visual input, but this information may be represented in other frequency bands.

NEW & NOTEWORTHY Neural oscillations in the alpha frequency band support selective attention to visual items and maintenance of their spatial locations in human working memory. Here, we investigate how eye movements disrupt representations of item locations held in working memory. Although it was not possible to recover item locations from alpha during eye movements, retained location information could be recovered from select lower frequency bands. This suggests that during eye movements, stored spatial information may be represented in other frequencies.

alpha; eye movements; inverted encoding model; spatial representations; working memory

INTRODUCTION

Goal-directed behavior requires a cognitive system that can generate and maintain stable mental representations of task-relevant objects and locations in the visual environment despite interruptions to continuous visual input. Behaviorally relevant items and locations are coded in patterns of brain activity. Selective attention to object locations, as well as the encoding and maintenance of locations in working memory (WM) is supported by patterns of oscillatory activity in the alpha frequency band measured with electroencephalography (EEG; 1–6, 22). Recent data suggest that stored representations of locations coded in the alpha band can be altered by different manipulations, such as

Correspondence: T. Bullock (tombullock@ucsb.edu).
Submitted 2 July 2021 / Revised 21 March 2023 / Accepted 22 March 2023

redirection of spatial attention during retention (5), pattern masking, eye closure, and eye blinks (2). The goal of the present study was to investigate how a predominant type of visual interruption—voluntary eye movements—affects the maintenance of spatial location information in alpha.

Object locations are unlike other object features (e.g., color) in that they can be maintained in the absence of the object by continuously directing spatial attention, either covertly or with eye movements, toward the stored location. Given that patterns of oscillatory activity in alpha support both ongoing spatial attention and maintenance of object locations (e.g., see Refs. 3 and 6) this raises the possibility that a common mechanism might be responsible for both spatial attention and spatial WM. There is recent evidence, however, that a distinct pattern of alpha activity can emerge to support the maintenance of behaviorally relevant locations when participants are required to close their eyes during the retention period of a spatial WM task when compared with keeping their eyes open (2). This work also demonstrated that when continuous spatial attention to a remembered location was interrupted by eye blinks or backward masking of the object, the fidelity of location representation in alpha is temporarily degraded (2). Together, these data suggest that while attended and remembered locations may be coded in alpha activity in more than one way depending on the task; alpha, nevertheless, is involved in both spatial attention and spatial WM. However, while eye-closure and masking disrupt the continuous flow of visual information, they do not necessarily disrupt the internal mapping of spatial information, leaving the possibility that alpha may reflect a continuously maintained retinotopic map or a trace of the map that remains when the eyes are closed. This raises the first question of whether alpha oscillations support location-specific representations when continuous visual input is disrupted by shifts of the retinotopic map, such as those that occur with eye movements.

Object locations also appear to be such an integral component of WM that they are encoded and maintained along with nonspatial features regardless of whether space is behaviorally relevant (7–11). In one study, participants completed a single-item WM task where a colored item was presented at different locations and they were required to report the color of the memorandum after a brief delay period (7). Patterns of alpha oscillatory activity coded object locations during the delay period despite participants only being required to report color, suggesting that item locations are coded in alpha regardless of whether they are to be explicitly remembered or not. However, the extent to which behavioral relevance influences the persistent coding of spatial information in alpha when continuous visual input is disrupted is currently unknown. This raises a second question of whether alpha oscillations support coding of item location during disruptions of continuous visual input even when location is not the to-be-remembered feature.

To investigate these questions, the present study examined how eye movements modulate stored location-selective representations in alpha. Eye movements disrupt continuous sampling of information from the visual environment by changing the mapping of external space onto the retina and redirecting overt spatial attention (12–15), but without removing external visual input as per previous manipulations (2). Maintaining a stable spatiotemporal (world centered) view of the world requires the retinotopic (eye-centered) coordinates of items in the visual environment to be continuously remapped across eye movements. Earlier behavioral and human neuroimaging work has demonstrated that the visual system's native representation of spatial attention is retinotopic, with evidence that the retinotopic trace of a previously attended location persists throughout the visual cortex after a saccade (16–18). There is evidence tying alpha oscillations to the timing of saccades during the exploration of a visual scene (19); however, the role of alpha in the representation and remapping of stored spatial items following a saccade has not been investigated.

Here, participants completed trials of a modified delayed spatial estimation task (6) while we recorded EEG at the scalp and used gaze-contingent eye tracking to ensure that eye movements were made as instructed. To investigate our first research question—whether alpha oscillations support location-specific representations when continuous visual input is disrupted—participants either maintained fixation at the center during the retention period, thus allowing continuous sampling of the to-be-recalled location, or they executed a sequence of guided eye movements. The purpose of having participants either fixate at the center or move their eyes during retention was to enable comparison of spatial representations in alpha when the retinotopic map is maintained (fixate at center) or changed (eye movements). In *experiment 1* (*E1*), a sample of participants made a sequence of guided eye movements in rapid succession during the retention period. Here, the goal was to test whether the remembered spatial location could be reconstructed despite the continuous disruption to the flow of visual information during retention. In *experiment 2* (*E2*), a new sample of participants made fewer eye movements during the retention period. Here, the goal was to test whether the remembered spatial location could be reconstructed when the eye gaze was relocated from fixation (where the initial spatial encoding occurred) and was stabilized for an extended period in a new location. If alpha continues to maintain spatial representations during eye movements this would be evidence that alpha is a mechanism of WM and not simply attention. However, if alpha does not maintain spatial representations during eye movement, and a memory of the location remains afterward, this would indicate that alpha is more closely aligned with visual attention and not WM except when the two processes overlap due to task demands. To investigate our second research question regarding whether alpha-based location coding interacts with behavioral task relevance, participants also completed trials of the task where they recalled a nonspatial feature (color) of the object (7) and either maintained fixation or made eye movement.

First, alpha lateralization was examined to confirm that shifts in posterior alpha were driven by stimulus location as expected, but this lateralization was disrupted when participants were required to maintain spatial information and to not make eye movements. Next, spatial patterns of oscillatory activity recorded at the scalp during this task were used as inputs to the IEM and model generalization schemes (6, 20, 21) were then applied to assess the effects of eye movements on location-selective representations in WM. Although investigating alpha was the primary goal of this study, exploratory IEM analyses were also conducted using other frequency bands to

explore alternative mechanisms for the representation of location in WM during eye movements. To our knowledge, there is currently no evidence from IEM studies in humans that frequency bands outside alpha play a role in the persistent spatial coding of retained information in WM (e.g., 6, 22); however, it is possible that other frequency bands might be recruited to maintain spatial information in WM under specific task demands that require increased cognitive control. Theta oscillations (~4–7 Hz) are thought to be involved in cognitive control and are a potential candidate (23). For example, theta oscillations play a role in the coordination and integration of the different brain regions involved in WM (24, 25) and specifically in orchestrating posterior alpha during multitask sequences that tax WM (26). However, it is also possible that the contribution of theta during WM retention does not result in spatial patterns across the scalp that can be detected by the IEM, hence the lack of evidence from previous work.

METHODS

Experiment 1

Both *experiment 1* (*E1*) and *experiment 2* (*E2*) apply a similar methodological approach to previously published work from our laboratory (1, 2). As a result, there is overlap in the phrasing and sentences used to describe techniques that are common across papers.

Participants.

Twenty-five undergraduate students (mean age = 19.9, 10 females, 2 left-handed) were recruited from the University of California, Santa Barbara Psychological and Brain Sciences research pool. Participants either received research participation credit or $12/h compensation for their time. Participants reported normal or corrected-to-normal vision and no color blindness. Informed consent was collected at the beginning of each session. All procedures were approved by the UCSB Human Subjects Committee and by the US Army Research Lab Human Research Protection Office.

Stimuli and procedure.

Each participant completed two testing sessions on two separate days. Sequential sessions were separated by a minimum of 24 h. Each participant was positioned in a chin rest 120 cm from a monitor (19 in. ViewSonic E90f CRT) and an eye tracker (Eyelink 1000 plus, SR Research Ltd., Mississauga, Ontario, Canada) was positioned 60 cm from the right eye. In each session, participants completed variants of a delayed spatial estimation task (2, 6). The task was controlled using the Psychophysics Toolbox (27) for MATLAB (v.2013b, The MathWorks, Inc., Natick, MA). The common trial structure is as follows (Fig. 1). Each trial began with a small dark gray fixation dot presented at the center of the screen (subtending 0.2° visual angle), along with a small green dot (subtending 0.4° visual angle) indicating current eye-gaze location. The participant initiated the trial by aligning the current-gaze dot with the fixation dot and pressing the space bar. The fixation dot then turned gray to indicate the successful initiation of the trial. After a variable interval (0.6–1.5 s), a colored stimulus appeared (0.25 s duration; subtending 1.6° visual angle) on the circumference of an imaginary circle centered on fixation (subtending 4° visual angle). The stimulus then disappeared and after a retention period (1.75 s), the participant was prompted to recall a specific characteristic of the stimulus, contingent on task instructions.

Two independent task manipulations were implemented to assess the impact of eye movements on spatial representations in WM. For the eye-movements manipulation, participants were either required to maintain fixation at the center during the retention period ("fix" conditions) or they were required to make discrete eye movements guided by location changes of the fixation dot ("move" conditions). In the "move" conditions, the fixation dot changed location three times on a fixed schedule during the retention period. Each new dot location appeared on an imaginary circle centered on fixation (subtending 4° visual angle). For the first location change (0.5s poststimulus onset), the fixation dot moved to a new pseudo-random location. For the second location change (1 s poststimulus onset), the dot moved to the location on the imaginary circle directly opposite the first location. For the third location change (1.5 s poststimulus onset), the fixation dot returned to the center. The three eye-movement cues are abbreviated to EM1 (eye-movement cue 1), EM2 (eye-movement cue 2), and RF (return eye gaze to fixation cue) throughout the text and figures. For the memory manipulation, participants were either prompted to recall the spatial location or the color of the stimulus ("spatial" or "color" conditions, respectively). On "spatial" trials, a gray response wheel appeared and the participant used the mouse cursor to indicate the recalled stimulus location. On "color" trials, a color wheel appeared and the participant used the mouse cursor to indicate the recalled stimulus color. The color wheel position was randomized on each trial so that participants could not map specific screen locations with color space. Both the location and color wheels subtended 4° visual angle. Randomization of the mouse cursor starting location prevented participants from making preparatory mouse movements during the retention interval. The next trial was initiated immediately after the participant made a response.

Stimulus location and fixation dot location were determined by pseudo-randomly selecting a location from one of eight bins relative to fixation (0°, 45°, 90°, 135°, 180°, 225°, 270°, and 315°) and jittering the location within the bin between 1° and 44°. Stimulus color was determined in an analogous manner, such that color space was parsed into 360 equal chunks and divided into eight equally spaced bins, and then the stimulus color bin was pseudo-randomly selected from the eight bins and the stimulus color randomly jittered within the bin between 1° and 44°. The "Memory" (spatial vs. color) and "Eyes" (fixate vs. move) variables were factorially combined to create four conditions: Spatial/Fix, Spatial/Move, Color/Fix, and Color/Move. Condition was blocked, and participants completed four blocks of 64 trials per condition in each of the two sessions, with order counterbalanced within a session. As condition was blocked, participants knew what the to-be remembered information was (location or color) such that only location or color needed to be attended and retained.

Gaze-contingent eye tracking was implemented during prestimulus, stimulus, and retention periods in all conditions. During the prestimulus and stimulus periods, if the eye-tracker detected a blink or a gaze deviation greater than 1.6° of visual angle from fixation, the trial was considered

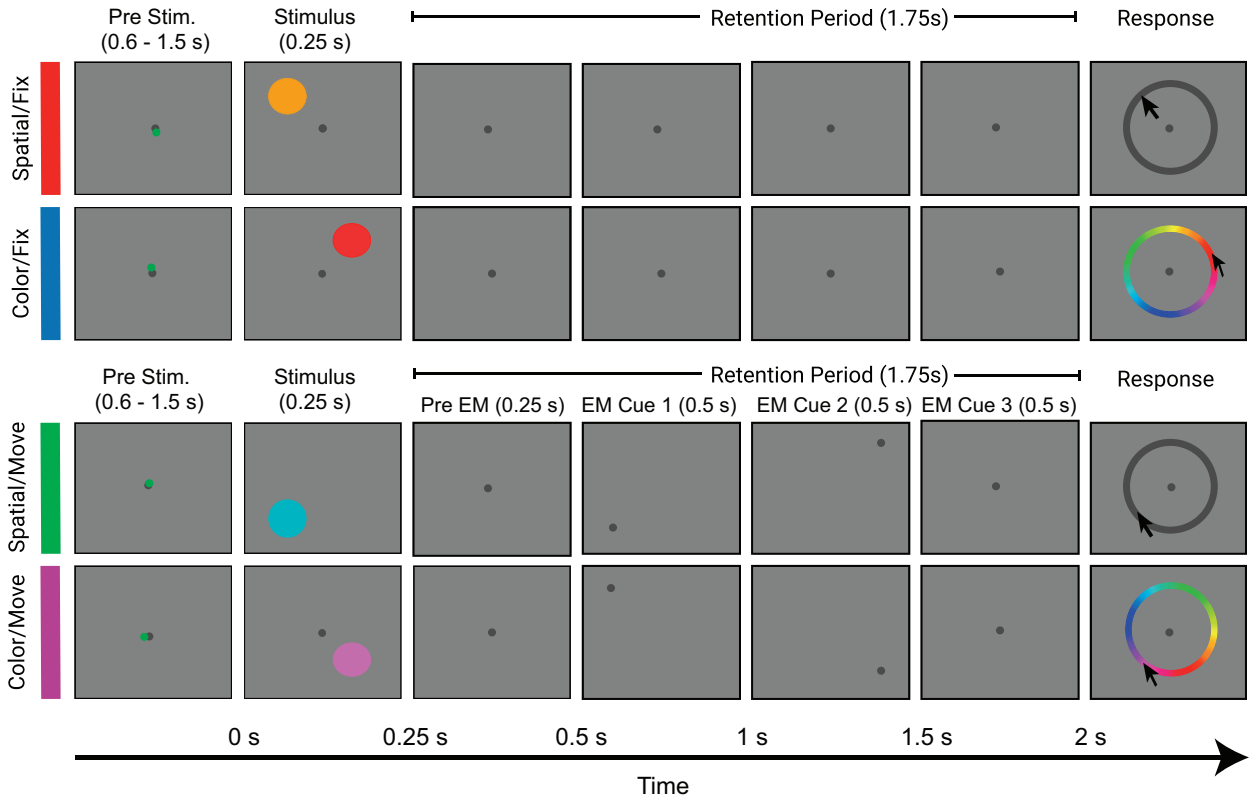

Figure 1. Delayed estimation task (*experiment 1*). Schematic examples of the trial procedure for each of the four conditions. Each trial began with the participant aligning a green dot reflecting their current eye position with the dark gray fixation dot and pressing the space bar once fixation was achieved. The green dot then disappeared and after a brief delay (jittered between 0.6 and 1.5 s) the probe stimulus was presented (0.25 s). The participant was required to retain either the location ("spatial" conditions) or the color ("color" conditions) of the probe throughout the 1.75 s retention period. In the "fixate" conditions, the participant maintained gaze at the center throughout the entire retention period. In the "move" conditions, the participant was required to track the position of the dot as it moved to the first location (eye-movements cue 1, EM1 Cue), the second location (eye-movements cue 2, EM2 Cue) and then returned to fixation (RF Cue). At the end of the retention period, the participant either reported the recalled probe spatial location or color by clicking on a response wheel. Conditions were blocked and order was fully counterbalanced across participants.

invalid, immediately terminated and the next trial began after a brief delay. This rule also applied to the retention period in the "Fixate" conditions. In the retention period for the "Move" conditions, the eye-tracker monitored each new fixation dot location for an eye-gaze position within 1.6° of the visual angle of the dot, to ensure that participants were moving their eyes as instructed. If correct eye movements were not detected at any point in the retention period then the trial was terminated. The 1.6° tolerance was chosen during pilot testing of the task as the smallest tolerance that allowed participants to proceed without incorrectly terminating an excessive number of trials due to eye gaze tracking error. Terminated trials were repeated by the participant at the end of each block of trials, thus ensuring that the full complement of 64 valid trials was collected per block. In total, 2,048 valid trials were collected per participant across the two experimental sessions, with each session consisting of 1,024 trials (64 trials per block × 4 blocks × 4 conditions). Condition order of presentation was counterbalanced between participants and was identical for each of the participant's two sessions.

Behavioral data modeling.

The MemToolbox (28) was used to model performance on the delayed estimation task. For each participant, the error between the recalled and actual stimulus location or color was computed for each trial and a standard mixture model with bias was applied to obtain measures of recall precision and guess rate.

EEG acquisition and preprocessing.

EEG was recorded at the scalp with an Active Two system (BioSemi, Amsterdam, the Netherlands) comprised of 64 Ag-AgCl sintered active electrodes placed in accordance to the 10-20 system on an elastic cap (Electro-Cap, Eaton, OH). Additional electrodes were placed 1 cm lateral to the left and right canthi (horizontal), above and below each eye (vertical), and on the right and left mastoids. EEG data were sampled at 1,024 Hz and referenced to the average mastoid signal.

EEG data preprocessing.

EEG data were processed offline with custom scripts that use functions from the EEGLAB toolbox (29) and MATLAB (v.2018a, The MathWorks, Inc., Natick, MA). The EEG data were downsampled to 256 Hz (EEGLAB function *pop_resample*) to reduce processing and memory demands. The data were then re-referenced to the average mastoid signal, a low-pass filter at 80 Hz was applied (EEGLAB function *pop_eegfiltnew*) and then the Automatic Artifact Removal (AAR)

toolbox (30) was applied to remove ocular artifacts. The data were then epoched from 0.5 s before stimulus onset to 0.5 s after retention period offset (i.e., −0.5 s to 2.5 s). The 0.5 s of additional data at either side were included as a buffer to prevent edge artifacts from contaminating the data at the later bandpass filter stages. For IEM analyses, the data were baseline corrected to the mean of the epoch. For alpha lateralization analysis, the data were baseline corrected to the prestimulus baseline period (−0.5 to 0 s).

Next, noisy electrodes were identified via visual inspection and removed [electrode rejection (means ± SE) = 2.50 ± 0.36%] and threshold-based artifact rejection (EEGLAB function *pop_eegthresh)* was applied to remove epochs in remaining electrodes with amplitudes that exceed ± 150 μV (trial rejection per condition: spatial/fix = 1.58 ± 0.29%, color/fix = 1.11 ± 0.28%, spatial/move = 1.85 ± 0.41%, color/move = 1.53 ± 0.23%). To avoid potentially introducing bias into the IEM, if an electrode was bad for one session or one condition, we removed it from all sessions and conditions for that participant. Noisy electrodes were interpolated for alpha lateralization analyses. This ensured that the electrode array remained consistent across participants, meaning that we were able to generate scalp topography plots averaged over all participants and compute alpha lateralization indices using the same clusters of electrodes for all participants (see *Alpha-lateralization analyses*). Noisy electrodes were excluded and not interpolated for the IEM analyses to avoid unnecessarily adding reconstructed electrode data into the model (see *Inverted encoding modeling*).

Spectral analysis.

A third-order Butterworth filter (MATLAB function *butter*) was applied to the clean, epoched data with a bandpass of 8–12 Hz to isolate oscillatory activity in the alpha band. A Hilbert transformation (MATLAB function *Hilbert*) was then applied to the bandpass filtered signal to extract values for instant amplitude and phase. The data were then parsed by location bin. Artifact rejection can result in uneven numbers of trials per location bin, so it was necessary to equalize the number of trials per bin to avoid introducing bias into the analyses. To do this, the location bin with the minimum number of trials was identified and a subsample of trials with size ($n - 1$) was randomly selected from each location bin. Selecting $n - 1$ trials was done to ensure that a random subsample of trials was selected from every bin, including the bin with the minimum number of samples. For both alpha lateralization analyses (see *alpha-Lateralization analyses*) and the primary IEM analyses (see *Inverted encoding modeling*), total alpha power (i.e., alpha power that reflects ongoing oscillations not phase-locked to a specific stimulus event) was then calculated by taking the square of the absolute of the Hilbert transformed values.

Alpha-lateralization analyses.

The topographic distribution of alpha across the scalp is modulated when attention is directed toward stimuli located on the left- or right-hand side of the visual field (4, 31, 32). To assess the extent to which this effect was present in our data, we computed an alpha lateralization index by entering the mean of alpha power averaged across lateralized parieto-occipital and occipital electrode sites (PO3/4, PO7/8, O1/2) into the following equation:

$$\text{Alpha Lateralization Index} = \frac{\text{ipsilateral power} - \text{contralateral power}}{\text{ipsilateral power} + \text{contralateral power}}$$

Inverted encoding modeling.

Data were submitted to an IEM to estimate spatially selective neural population response profiles based on topographical patterns of alpha activity across the scalp (2, 5–7). This encoding model assumes that the neural responses can be modeled as information channels (33). First, the model estimates the extent to which the linear combination of a priori canonical channel responses (i.e., basis set) captures the underlying structure of the observed data, yielding a set of regression weights for each channel for each EEG electrode. In other words, these weights describe the contribution of each EEG electrode to each location-specific channel. Next, the model uses the weights to estimate the channel response from the observed data. The resulting channel response functions can then be quantified to estimate the spatially selective response (see *Quantifying spatially selective representations*).

Spectral data were split into location bins and trial counts were equalized across bins as described in *Spectral analysis*. Each location bin was then subdivided into three randomly selected sets of trials and averaged across trials to create three averaged trials for each location bin. The averaging helps to improve signal-to-noise ratio and reduce computational demand. These 24 averaged trials (8 locations × 3 averaged trials) were then entered into the IEM. To ensure that model outcomes were not influenced by idiosyncratic trial selection, the trial selection procedure was repeated 10 times, randomly selecting different trials on each iteration and entering them into the subsequent IEM.

The IEM was run for each individual sample over the trial epoch (256 Hz EEG sampling rate × 2.5 s = 640 sample) within each condition for each participant. The IEM was validated using a k-fold approach where $k = 8$. The averaged trials were grouped into eight folds, each consisting of one averaged trial per location bin. The model was trained on seven folds and tested on the single "left out" fold. This procedure was then repeated so that each fold served as the test fold. Critically, the model was trained on an equal number of trials drawn from the four conditions to generate a "fixed" encoding model. Training the model across all conditions, as opposed to training a separate model for each condition, helps to reduce the possibility that observed differences in spatial selectivity between conditions may just reflect differences in signal-to-noise ratio between conditions (33–36).

For each participant and condition, m represents the number of EEG electrodes in each data set, n_1 represents the number of trials in the training set (7 folds of 8 averaged trials) and n_2 represents the number of trials in the testing set (1 fold of 8 averaged trials). Let j be the number of hypothetical spatially selective response channels (C_1, $j \times n_1$), composed of half-sinusoidal functions raised to the seventh power as the basis set. Here, the basis set comprised eight equally spaced locations (i.e., $j = 8$). B_1 ($m \times n_1$), represents the training set and B_2 ($m \times n_2$) represents the test set. A standard implementation of the general linear model (GLM) was then used to estimate the weight matrix (W, $m \times j$) using the basis set (C_1). More specifically, using the GLM:

$$B_1 = WC_1.$$

The ordinary least-squared estimate of W can be computed as follows:

$$\hat{W} = B_1 C_1^{\mathrm{T}} \left(C_1 C_1^{\mathrm{T}}\right)^{-1}.$$

Using the estimated weight matrix ($\hat{W}$) and the test data (B_2), the channel responses (C_2, $j \times n_2$) can be estimated by the following:

$$\hat{C}_2 = \left(\hat{W}^T \hat{W}\right)^{-1} \hat{W} B_2.$$

After the $\hat{C}_2$ was solved for each location bin, the channel response function (CRF) for each averaged trial was then circularly shifted to a common stimulus-centered reference frame (degrees of offset from the channel's preferred location bin), and the centered CRFs were averaged across trials. The model was then repeated for each time sample. To safeguard that the outcome of the model was not influenced by an idiosyncratic selection of trials, the model was repeated ten times, with a randomized selection of trials being entered into the IEM on each iteration and the final centered CRF was computed by averaging over the 10 iterations.

The IEM procedure was also repeated with randomly permuted location bin labels. Here, 10 iterations of the model were computed with a set of randomly permuted bin labels as per the trial randomization protocol described in the previous paragraph. This process was then repeated five times, using a new shuffled set of permuted labels for each iteration. The CRFs were then averaged across all iterations and permutations to generate "permuted" CRFs. Randomizing the location bin labels should eliminate spatially selective response and result in flat channel response profiles. These permuted CRFs were then used as a baseline for hypothesis testing.

Temporal generalization of IEM.

To observe intraconditional temporal generalization of spatially specific patterns of alpha activity, the IEM training and testing procedure described earlier was applied to every combination of time points within each condition. To reduce computation time and the total number of comparisons, the data were downsampled to 64 Hz before modeling. As detailed in the previous analysis, the generalization analyses were also computed with both real and permuted location bin labels for the purpose of hypothesis testing.

Quantifying spatially selective representations.

To quantify spatial selectivity, the estimated channel responses were folded around 0° offset, transforming responses from [−135°, −90°, −45°, 0°, 45°, 90°, 135°, 180°] into [0°, 45°, 90°, 135°, 180°] by averaging the response at corresponding offsets (±45°, 90°, and 135° were averaged; 0° and 180° were not). Slope was then computed as the linear regression weight of alpha power across offset. Larger slope values indicate greater spatial selectivity.

Broadband IEM analyses on total and evoked spectral power.

The primary focus of the analyses presented thus far has been on total alpha power, as previous work has shown that this is where spatially selective information is represented during the retention period (e.g., 2, 5, 6). However, it is also possible that information on spatial location may be represented in other frequency bands outside of alpha, and these representations may be modulated by the unique eye movements or memory manipulations presented in this study. Furthermore, previous work has shown that while spatially specific representations are present in evoked spectral activity after stimulus onset, these representations do not sustain for the duration of the retention period (5, 6), perhaps because evoked activity fades after the initial phase-locking event (i.e., probe stimulus onset). In the present study, the "move" conditions require participants to make three large eye movements during the retention period. Saccades are known to evoke phase resets across a range of frequency bands (37–40) and it is possible that these resets could reactivate or boost the signal of the stored representation. To explore these possibilities, broadband IEM analyses were computed for both total and evoked power. Total power was computed as before, by taking the square of the absolute of the Hilbert transformed values and entering these data into the model before generating sets of averaged trials. As such, total power represents all ongoing activity in a defined frequency band irrespective of the relationship of that activity to specific phase-locking events (e.g., stimulus onset). Conversely, evoked power was computed by taking the square of the absolute of the Hilbert transformed values after generating sets of averaged trials. The evoked activity reflects activity that is phase locked to a specific event (e.g., stimulus onset) so calculating the square of the absolute values after trial averaging means that only activity with consistent phase across trials remains and is entered into the subsequent model.

The same processing and modeling steps described in *Spectral analysis*, *Inverted encoding modeling*, and *Quantifying spatially selective representations* were applied to cleaned, epoched total, and evoked data bandpassed in 1 Hz chunks between 1 and 30 Hz using a third-order Butterworth filter (MATLAB function *butter*). Data from the same set of artifact-free electrodes were entered into the IEM for each 1 Hz frequency band. As per the generalization analyses, the data were downsampled to 64 Hz to reduce computation time.

Eye-movements error analysis.

Gaze contingent eye tracking ensured that participants directed their gaze as instructed throughout each trial and condition in the experiment. However, despite careful calibration and minimizing head movement by positioning participants on head support, there were sometimes discrepancies between the actual eye-gaze position and the position detected by the eye-tracker, particularly during the fast eye movements that were required in the "move" conditions. To avoid incorrectly aborting trials due to eye-tracker error, it was necessary to set up fairly large regions of interest (ROIs) around the two eye-movements fixation cues (1.6° of visual angle). To confirm that participants were moving their eyes into these ROIs, the minimum Euclidian distance between the eye-gaze cue and eye-gaze position within eye-movements *window 1* (0.5–1 s) and *window 2* (1–1.5 s) was computed for both "move" conditions, as well as the timing of the minimum error within each window.

Hypothesis testing.

Bayes factors (BF) were calculated for the purpose of inferential statistics (41–43) using functions from the Bayes Factor Toolbox in R (44), which uses a Cauchy prior. According to various guidelines, a BF between 1 and 3 indicates "anecdotal evidence" for H1, between 3 and 10 indicates "moderate" evidence, between 10 and 30 indicates "strong" evidence, and >30 indicates "very strong" evidence (41, 42, 45, 46). In this manuscript, BF > 3, BF > 10, and BF > 30 are used to indicate moderate, strong, and very strong effects, respectively. Very large BF factors are represented as BF > 1,000.

To test for alpha lateralization, BF *t* tests (R function *ttestBF*) were computed against zero. To test the reliability of the spatially selective channel responses, BF paired *t* tests (R function *ttestBF*) were computed for each sample over time comparing the slopes of the real and permuted channel response estimates. This approach was applied to the initial "within" IEM analyses as well as the intra- and intercondition temporal generalization analyses. To test for differences between conditions, BF ANOVAs (R function *anovaBF*) with the factors "eyes" (fixated vs. moved) and "memory" (spatial vs. color) were computed, comparing the slopes of real channel estimates at each time point.

Several analyses presented here involve repeated comparisons at multiple time points, which raises the specter of increased inferential error. However, it should be noted that Bayesian inference, even without correcting for multiple comparisons, is more conservative than frequentist inference, and models are less likely to result in false confidence (47). Furthermore, robust effects are clearly present at multiple time points and no inference relies on effects at single, disjointed time points, but rather a pattern of effects over time. Any inferences are further strengthened by the use of IEM parameters based on permuted data for comparisons, which yields a more realistic null for our comparisons, and that reported parameters are averaged over multiple repetitions of the IEM. These features should help mitigate peculiarities in the data at a given time-point or sample of trials.

Experiment 2

E1 required three eye movements to be made in fairly rapid succession during the retention period (3 cues, 500 ms between each cue). The EEG activity recorded at the scalp throughout this period was therefore impacted by ocular artifacts and patterns of alpha activity that were continuously shifting along with eye movements. This meant the patterns of data being fed into our model were unstable, which may explain why we were unable to reconstruct CRFs during retention in the eye-movements conditions. This raises the question of whether it is possible to reconstruct CRFs when eye gaze is relocated from central fixation (where the spatial information was initially encoded) and then held constant in a new position, thus allowing brain activity to be recorded in a relatively stable state with minimal ocular artifacts. We address this question in *E2* by requiring participants to execute a single guided eye movement away from the center during the retention period after they have encoded the memorandum, and then move back to the center just before the end of the retention period.

A new sample of participants was tested for *E2*. The data collection, recording, and analysis techniques applied in *E2* were identical to those described in *E1*, expect for the modification to the task.

Participants.

Twenty-five undergraduate students (mean age = 20.5 yr, 19 females, 1 left-handed) were recruited from the University of California, Santa Barbara Psychological and Brain Sciences research pool. Participants either received research participation credit or $20/h compensation for their time. Participants reported normal or corrected-to-normal vision and no color-blindness. Informed consent was collected at the beginning of each session. All procedures were approved by the UCSB Human Subjects Committee and by the US Army Research Lab Human Research Protection Office. One participant was excluded due to excessively noisy EEG data and another was excluded because they performed the task incorrectly in one condition.

Stimuli and procedure.

The stimuli and protocol were identical to *E1* with the exception of the eye-movements protocol in the "move" conditions. In *E1*, the fixation dot changed location three times during the retention period, requiring participants to make a total of three eye movements. In *E2*, participants were only cued to make two eye movements, at 0.5 s and 1.5 s poststimulus, essentially providing ~1 s of stable gaze-off-center fixation time (Fig. 2).

EEG preprocessing.

The EEG data were submitted to the same preprocessing pipeline as in *E1*. For completeness, artifact rejection statistics are reported here. Noisy electrodes were identified via visual inspection and removed [electrode rejection (means ± SEM) = 8.4 ± 0.91 electrodes] and threshold-based artifact rejection (EEGLAB function *pop_eegthresh)* was applied to remove epochs in remaining electrodes with amplitudes that exceed ± 150 μV (trial rejection per condition: spatial/fix = 7.68 ± 1.26%, color/fixate = 7.31 ± 1.33%, spatial/move = 4.75 ± 0.79%, color/move = 4.60 ± 0.67%).

RESULTS AND DISCUSSION

Experiment 1

Precision and guess rate are modulated by memory and eye-movements manipulations.

Participants were less precise and made more guesses when required to recall color when compared with the recall of spatial location (BF Memory > 1,000; Fig. 3). Memory and eye-movement manipulations interacted to modulate location recall precision (BF > 1,000), such that requiring participants to make eye movements resulted in a large decline in location recall (BF > 1,000) but had no effect on color recall (BF < 1). Although there are differences between conditions, precision was generally high and guess rate low across all conditions, meaning that participants were engaged and performing the task as instructed across all conditions. The decline in spatial memory precision as a function of eye movements is broadly consistent with the drop in spatial recall accuracy observed

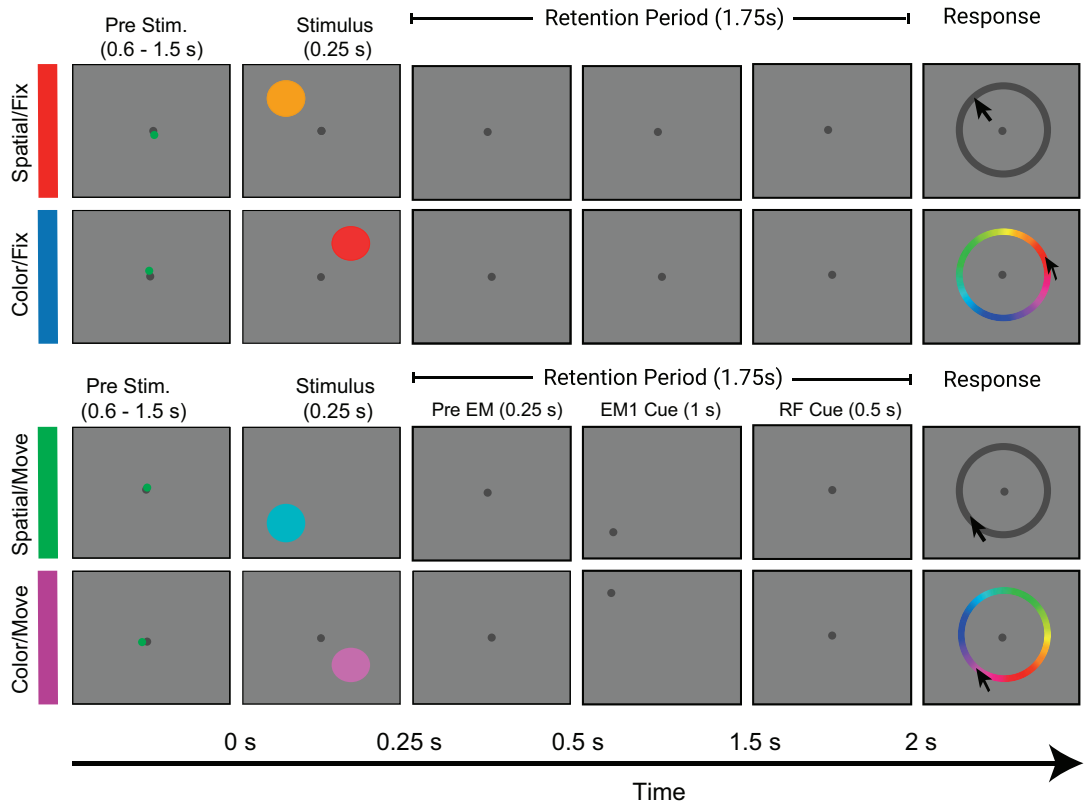

Figure 2. Delayed estimation task (*experiment 2*). Schematic examples of the trial procedure for each of the four conditions. The task stimuli and procedure were identical to *experiment 1* except during the retention period participants were just required to make one eye movements away from fixation [eye-movements cue 1 (EM1) Cue] and then return gaze to fixation [return to fixation (RF) Cue].

when participants are required to make visually guided saccades during the retention interval (17).

Alpha lateralization is modulated by eye movements and memory demands.

To determine the extent to which total alpha power lateralization across posterior scalp electrodes was disrupted by eye movements and memory manipulations, lateralization indices were averaged across critical time windows during stimulus presentation and retention. One-sample comparisons against zero were computed for each measure and time window to determine if there was evidence of lateralization. During stimulus presentation, alpha was lateralized across all conditions (all BF $>$ 30; Fig. 4). This observation is consistent with previous results (2, 4, 31, 48) and indicates that the current stimuli and task were modulating alpha topography as expected. However, lateralization was only consistent throughout the entire retention period in the spatial/fix condition (all BF $>$ 30), which implies that continuous spatial selective attention was directed toward the attended half of the screen throughout retention. In both the color/fix and color/move conditions, alpha was lateralized throughout eye-movements windows one and two (all BF $>$ 30), but not in the final eye-movements window (BF $<$ 3), suggesting that spatial information encoded in patterns of alpha is initially maintained but then fades later in the trial. In the spatial/move condition, lateralization was robust for the first and third eye-movements windows (BF $>$ 30) but not the second window (BF $<$ 3), indicating that spatial information held in alpha is disrupted by eye movements but can be recovered after the

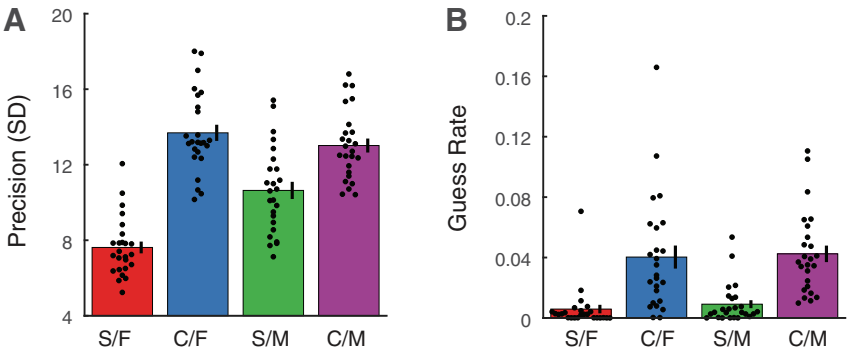

Figure 3. Behavior (*experiment 1*). Precision (SD in degrees from true location) (*A*) and guess rate (proportion of guess trials, i.e., where there was no memory; *B*) are shown for all conditions. In this and subsequent figures, the conditions are labeled as follows: S/F, Spatial/Fixate; C/F, Color/Fixate; S/M, Spatial/Move; C/M, Color/Move. Error bars = means ± SE.

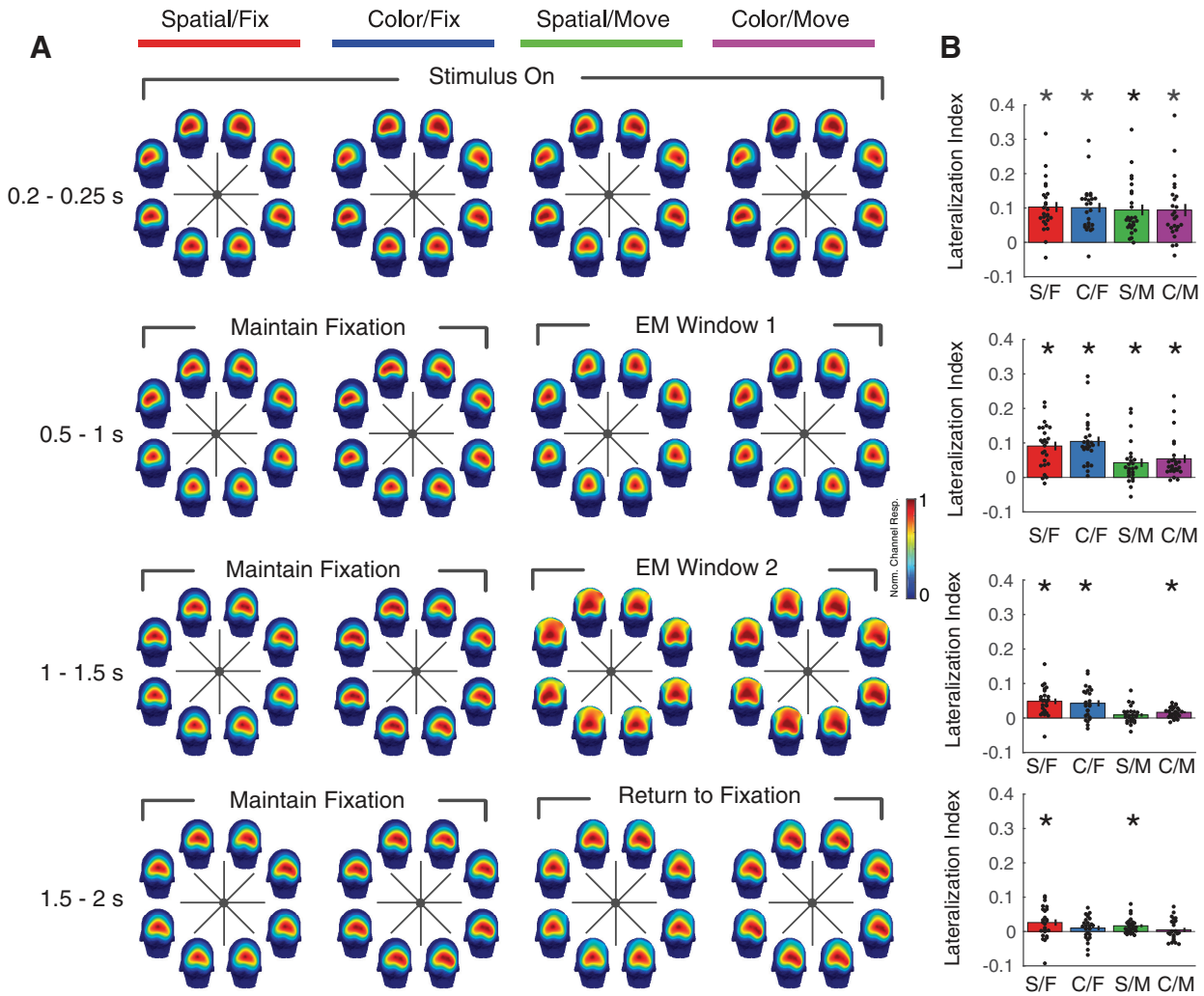

Figure 4. Alpha lateralization (*experiment 1*). *A*: topographic plots depict the distribution of alpha power across the scalp, averaged across trials and participants. Columns represent the four conditions. Rows represent the final 50 ms of stimulus presentation (0.2–0.25 s) and the retention period divided into three 0.5-s time windows that correspond to the three eye-movements windows in the "move" conditions [eye-movements cue 1 (EM1), eye-movements cue 2 (EM2), and return to fixation]. Note that the "fixate" conditions are divided into the same time windows so that alpha topography and lateralization can be compared between "fixate" and "move" conditions. The position of each head plot in the ring of plots reflects the mean activity across all trials where the stimulus was presented in the corresponding angular location bin. *B*: bar plots depict alpha lateralization indices for all conditions and time windows. Each row corresponds to the time window and topographic plots denoted in *A*. Higher values reflect greater lateralization. *Lateralization index significantly different to zero (Bayes factors, BF $>$ 3). Error bars = means ±SE. S/F, Spatial/Fixate; C/F, Color/Fixate; S/M, Spatial/Move; C/M, Color/Move.

cessation of eye movements and when gaze has returned to the original location.

Next, Bayes factor ANOVAs were computed to investigate differences in lateralization between conditions during each time window. Lateralization was consistent across conditions during stimulus presentation (all BF models $<$ 1) indicating that initial stimulus presentation had a consistent effect on alpha topography across all conditions. During the first and second eye-movements windows, statistical models containing memory and eye-movements factors, as well as the interaction, had large Bayes factors (BF $>$ 1,000), and follow-up pairwise comparisons confirmed reduced lateralization during both time windows in spatial/move when compared with spatial/fix (BF $>$ 30) and color/move when compared with color/fix (BF $>$3). No statistical differences in lateralization between conditions emerged during the third eye-movements window.

Together, these results confirm that shifts in posterior alpha were driven by stimulus presentation as expected, but alpha topography was only consistently lateralized during retention if participants were required to maintain spatial information and to not make eye movement.

Stored location-selective representations are degraded by eye movements.

Spatially selective CRFs were reconstructed from topographically specific patterns of total alpha power using the IEM technique. The slope of the reconstructed CRF indicates whether there is location-specific representation coded in patterns of brain activity that map onto the a priori basis set at a given time point. More specifically, a robust peak in the CRF at 0° channel offset falling off in a graded fashion with increasing offset indicates a location-selective response, whereas a flat CRF indicates that no

location-specific information is represented. CRFs for each condition are shown in Fig. 5*A*. The real and permuted CRF slopes with statistical comparisons are shown in Fig. 5*B* and the actual Bayes factor results are shown in Fig. 5*C*. In Fig. 5*D*, the Bayes factor ANOVA models comparing the slopes of the real data across conditions are shown for all combinations of main and interaction effects and in Fig. 5*E* the follow-up Bayes factor pairwise comparisons.

CRF slopes increased in all conditions following stimulus onset (Fig. 5*B*), with evidence for differences between real

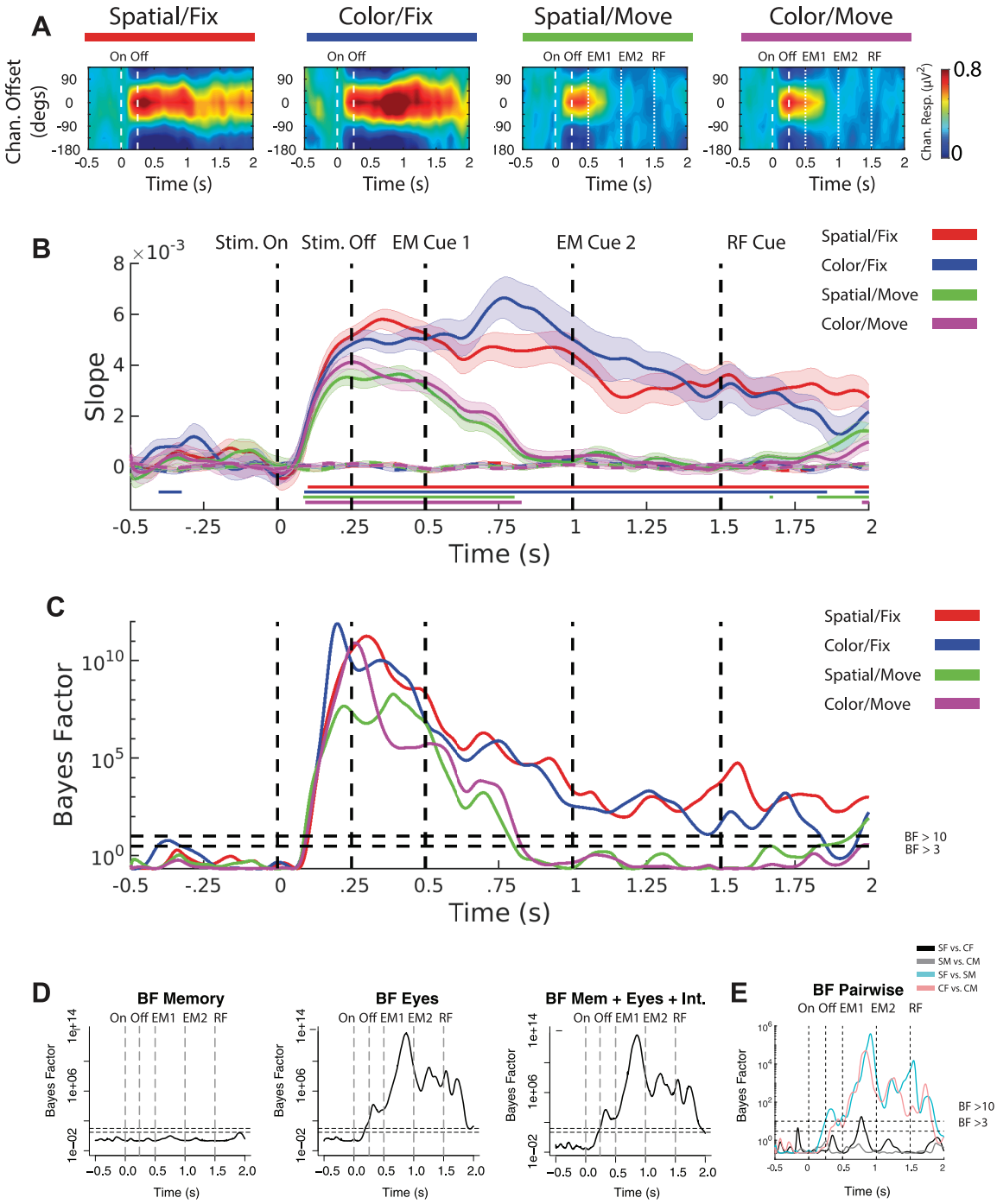

Figure 5. Modeling total alpha power (*experiment 1*). *A*: estimated channel response functions (CRFs) presented as heatmaps. *B*: CRF slopes, computed by folding each CRF at the peak channel offset at each time point and computing linear slope. Horizontal bars at base of plot indicate time points where there is moderate evidence for a statistical difference between each real CRF and its permuted baseline (Bayes factors, BF $>$ 3). *C*: actual BF values for tests comparing each real CRF and its permuted baseline. *D*: BF ANOVA model results comparing the "real" slope data across conditions (horizontal lower and upper dashed lines indicate BF $>$ 3 and BF $>$ 10, respectively). *E*: BF pairwise comparisons comparing the "real" slope data (horizontal lower and upper dashed lines indicate BF $>$ 3 and BF $>$ 10, respectively). Dashed vertical lines in all plots indicate stimulus onset (On) and offset (Off) and the three eye-movements cues [eye-movements cue 1 (EM1), eye-movements cue 2 (EM2), and return to fixation (RF)].

and permuted slopes present from ~100 ms onward, which is around the time when initial effects of covert shifts in spatial attention have previously been observed in evoked activity (49–52). Slope peaked just after stimulus offset in all conditions except in color/fix, where it spiked again early in the retention period (~0.75 s). The slope response to the stimulus was attenuated in eye-movements conditions when compared with fixation conditions, such that the initial stimulus-evoked response was lower and the decline during the early retention period was more rapid (see Fig. 5*C*, BF eyes and Fig. 5*D* from ~0.25 s onward). Modulation of stimulus-related processing in the eye-movements conditions may suggest that the anticipation of upcoming eye movements causes location to be represented at lower fidelity, possibly because spatial attention to the stimulus is more diffuse due to participants anticipating the onset of the randomly located impending eye-movements cue.

The slope in both spatial/fix and color/fix conditions remained different from the permuted baseline throughout the retention period, except for in the color/fix condition where it declined at ~1.85 s before rising again at the very end of retention ~1.95 s. Sustained activation throughout the retention period in the spatial/fix condition replicates previous results for this version of the task (2, 6) and indicates consistent maintenance of the location-selective representation. In contrast, while location information is initially spontaneously encoded and retained in the color/fix condition, the location representation fades before re-emerging in the final ~59 ms of retention, just before the onset of the color-wheel response screen. Spontaneous coding of spatial information during a nonspatial WM task is consistent with previous results that show robust CRFs for location during the retention of a color stimulus (7; *experiment 1*). In that case, there was a shorter retention period (1.2 s) and a robust sustained location selective response across the entire period. Conversely, the data reported here suggest that the sustained location response is time-constrained, and with a longer retention period (1.75 s) the response can become degraded. However, the re-emergence of the location representation in the final ~50 ms of retention and before response suggests possible binding of color and location.

After the initial peak following stimulus offset, slope declined at a faster rate in both eye-movements conditions when compared with fixation conditions. In the spatial/move condition, slope was not statistically different from the permuted baseline from ~0.80 s through to the very end of the retention period (~1.8 s), where the location-selective representation re-emerged. A similar pattern was also present in the color/move condition, but the representation did not re-emerge until even later (~1.95 s). Given the timing of the eye movements, this pattern suggests that the location-specific representation was initially disrupted by eye movements that forced the gaze to be directed away from fixation, but the representation then re-emerged when the eye gaze returned to fixation at the end of the retention period and the participant was presumably anticipating the forthcoming response screen.

Together, these data imply that eye movements disrupt the maintenance of spatial information as coded in alpha, but spatial representations can be reinstated at the cessation of eye movements regardless of whether these representations are coded spontaneously or because they are task-relevant.

Generalization analyses reveal neural coding dynamics during eye-movements windows.

The previous set of IEM analyses demonstrates that requiring participants to make large, guided eye movements away from fixation disrupts location-selective representations in the alpha band during the eye-movements time window. However, in both eye-movements conditions, the location representation then re-emerged when the eye gaze returned to the center and stabilized, and participants were able to accurately report the remembered location, albeit with less precision than when they were not required to move their eyes. Together, these results clearly indicate that a mental representation of the task-relevant spatial information is stored for later recall, but it is not possible to reconstruct this representation during the eye-movements period using the standard IEM procedure. This raises the question of what happens to the representation during the eye-movements period.

One possibility is that eye-movements-induced variability in the patterns of alpha activity being submitted to the IEM prevents the successful reconstruction of location-selective information. In the spatial/fix and color/fix conditions, stable eye gaze and continuous spatial attention to the object location during retention ensure that the distribution of alpha power across the scalp is reasonably consistent throughout each trial, thus the model is being trained and tested on stable patterns of alpha. In contrast, in the eye-movements conditions, eye gaze is redirected in pseudorandomized directions relative to the probe location several times during retention, requiring momentary shifts of spatial attention that disrupt patterns of alpha. These disruptions in global alpha topography as a function of eye movements result in lower alpha lateralization indices during the retention period (Fig. 4) when compared with the fixation conditions. Hence, in the previous set of IEM analyses, during the eye-movements window, the model is being both trained and tested on trial segments that have highly variable patterns of alpha, so any underlying stimulus-relevant patterns of activation are effectively washed out and the outcome is flat CRFs.

One way to examine this possibility is via a temporal generalization approach (21). This approach involves training and testing the model across all possible combinations of time points across the trial, so that time segments with more stable patterns can be tested against time segments with less stable patterns, and vice versa. Generalization models can be used to identify the extent to which specific neural codes are present across time within and between conditions. When generalization is present within or across conditions, this indicates that neural codes trained on the topographic pattern of neural activity in specific time windows can recover similarly reliable spatially selective patterns in other time windows and conditions. Here, if strong generalization is observed, then that is evidence for a common process, where a spatially selective representation can be recreated from a similar pattern of alpha at another time window or condition. Conversely, if weak or no generalization is observed, then there would be evidence that the representation is coded by a different topographical pattern of neural activity predicted by the basis set, i.e., a different process. In other words, poor generalizations indicate that the patterns of alpha measured across the scalp are different from one time window to another.

Within the spatial/fix condition, there was consistent encoding along the diagonal and extensive generalization both forward and backward in time from stimulus onset to the end of the retention period, indicating that a unitary process supports the spatially selective response during both stimulus presentation and retention intervals (Fig. 6, Spatial/Fix). This is consistent with previous results that demonstrate widespread generalization during encoding and retention periods when continuous spatial attention is uninterrupted (2). Within the color/fix condition (Fig. 6, Color/Fix), encoding along the diagonal was robust except for a brief drop close to the end of retention, consistent with the previous within-time-points IEM analysis (Fig. 5*B*). There was also widespread generalization throughout the stimulus and early retention periods, however, there was a failure to generalize later in the retention period. The generalization failure was very apparent when training on the final ~0.5 s of the retention period data and testing on the first ~1.0 s of the stimulus presentation. The failure was also observed when training on the first ~0.5 s of stimulus presentation and testing on the final ~1.0 s of retention period data, but this was less clear-cut, with some generalizations still occurring. Overall, this pattern suggests that the spontaneous coding of probe location and subsequent maintenance of location information are not supported by a unitary process within alpha and may in fact be coded by separate processes.

In both eye-movements conditions, there was no activation along the diagonal and no generalization beyond the first eye-movements window (0.5–1 s) in retention (Fig. 6, Spatial/Move and Color/Move). The generalization up to the end of the first eye-movements window is likely due to carry-over effects from the stable gaze period before the first eye-movements cue. Although the first eye-movements cue onsets at 0.5 s, it takes participants time to react and shift their gaze to the new gaze cue location, and then additional time for this to be reflected in shifts in the patterns of alpha. If the pattern did generalize, activation would be expected to stretch horizontally from around the stimulus period to the end of retention, but this is not the case, and reactivation of the representation is only observed at the cessation of eye movement in the Spatial/Move condition.

Evoked activity outside alpha may support location-selective representations during eye movements. Previous work has confirmed that while spatial information related to stimulus encoding can be represented in other frequency bands, stored location information appears to be exclusively represented in alpha band total power (2, 6). For this reason, the primary focus of the analyses presented thus far has been total alpha power. However, it is possible that location-selective representations may emerge in frequency bands outside alpha and/or in evoked power when continuous spatial attention is disrupted by eye movement. To explore this possibility, IEM analyses were computed from 1 to 30 Hz for both total and evoked power.

Total power analyses (Fig. 7*A*) confirmed that while the location was mainly represented in the alpha band during retention, there was some activation in theta and delta beginning during the stimulus presentation period and extending out beyond the stimulus offset. This activation was more robust and extended further into the retention period in conditions that required eye movements during retention, but was not sustained throughout the retention period as it was in alpha, suggesting that the enduring spatial representation in WM is exclusive to alpha when modeling total power.

Evoked power analyses (Fig. 7*B*) confirmed that location was represented in alpha and theta around the time of stimulus presentation in conditions where participants were instructed to maintain fixation throughout the trial, but then these representations faded following stimulus offset (~0.5 s). This is consistent with previous reports (5, 6). In the fixation conditions, location is represented at 10 Hz for the first half of the retention period but does not endure for the full 1.75 s. However, in the conditions that require eye movement during retention, there is a stronger spatially selective response in theta and delta around the stimulus period and a response specifically at 4 Hz that persists until the end of the spatial/move retention period and almost to the end of the color/move retention period. Enduring activity is also observed at 1 Hz, but this is not consistent throughout the entire retention period in either condition, and there is also a reactivation across 1–4 Hz at the very end of retention in the color/move condition. These effects suggest that spatially specific

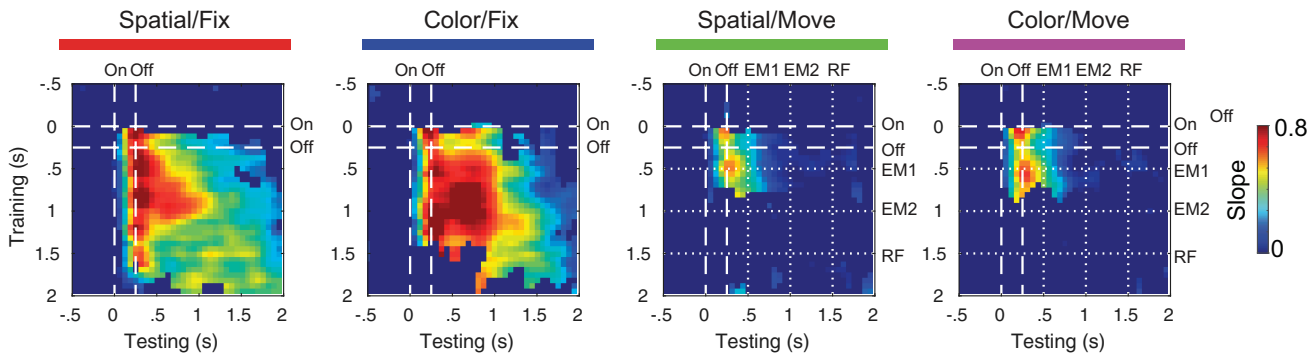

Figure 6. Temporal generalization of CRFs (*experiment 1*). The linear slopes of the channel response functions (CRFs) are plotted for each training and testing time-point, with greater slopes represented as hotter colors. Time-points where there is no statistical difference between real and permuted slope (Bayes factors, BF < 3) are plotted as uniform dark blue. Training and testing within each time-point [as per the previous inverted encoding modeling (IEM) analysis] is represented by activation along the diagonal stretching from the *top-left* to the *bottom-right* corners of each plot. Off-diagonal activations represent encoding endurance both backward in time (activations to the left of the diagonal) and forwards in time (activations to the right of the diagonal). Dashed horizontal and vertical lines indicate stimulus onset (On) and offset (Off) and the three eye-movements cues [eye-movements cue 1 (EM1), eye-movements cue 2 (EM2), and return to fixation (RF)].

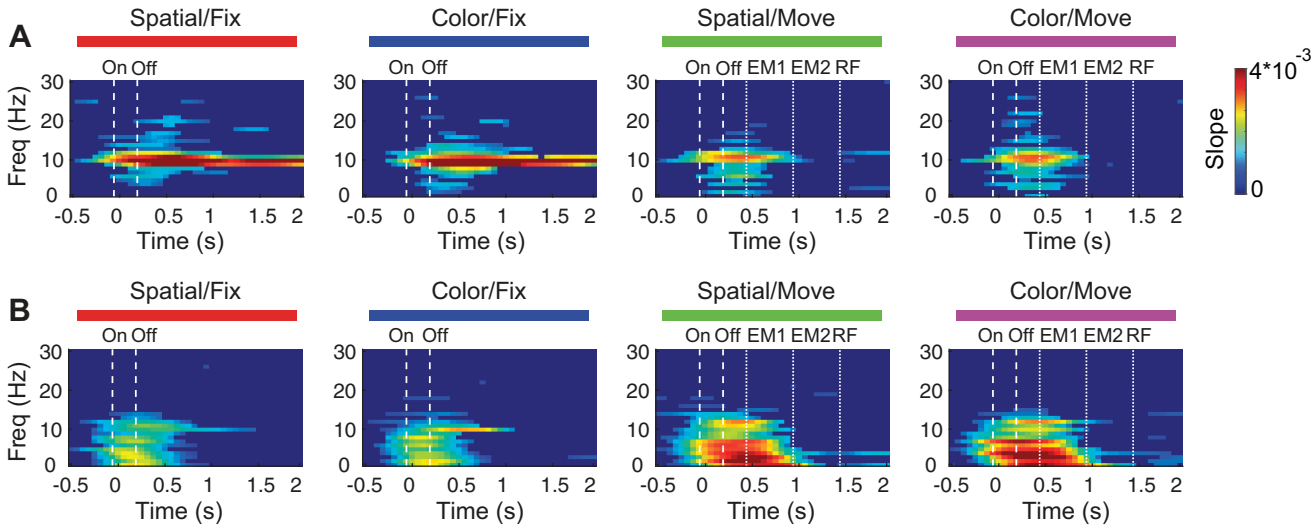

Figure 7. Tracking location-selective representations across a broad range of frequency bands for total (*A*) and evoked power (*experiment 1*) (*B*). Channel response functions (CRFs) slopes are plotted for each time sample across frequency bands 1–30 Hz. For each sample the slope of the real CRF is compared with the permuted baseline and if the resulting BF < 3 then the point is represented in uniform dark blue. Dashed vertical lines indicate stimulus onset (On) and offset (Off) and the three eye-movements cues [eye-movements cue 1 (EM1), eye-movements cue 2 (EM2), and return to fixation (RF)].

information may be carried in evoked activations in lower frequency bands such as theta and delta under circumstances where the focus of both overt and covert attention is temporarily disrupted by eye movements. Executing a series of eye movements while retaining the location of the spatial memorandum presumably requires greater cognitive control compared with just maintaining fixation. Lower frequency oscillations are known to play an important role in cognitive control (23) and in coordinating posterior alpha during multitask sequences in WM (26). Therefore, one possible explanation for these findings is that the lower frequency bands were sufficiently engaged during the eye-movements conditions such that the IEM became sensitive to the diverse spatial patterns of activity across the scalp. However, these effects observed during the retention period must be interpreted with caution, as they are only present in specific frequency bands spanning 1 Hz and are not as robust as the persistent results seen in total alpha. Nevertheless, the results suggest that the lower frequency bands may play a role in tracking the transient appearance of a spatial stimulus as well as the enduring representation of the stimulus when demands on spatial attention are increased.

Eye movements.

Gaze contingent eye-tracking ensured that participants shifted their eye gaze throughout each trial as instructed. However, due to an eye-tracker error it was necessary to set fairly liberal ROIs (1.6° visual angle radius) around the two eye-movements fixation cues to allow for discrepancies between the actual gaze position and the position detected by the eye-tracker. To determine the size of the error, the mean minimum Euclidian distance between the eye-gaze cue and eye-gaze position was computed and plotted (Fig. 8*A*) as well as the time within each eye-movements window when this occurred (Fig. 8*B*). Both eye movements were within the gaze cue ROI radius, indicating that participants were moving their eyes as instructed. However, the eye movements are relatively imprecise within the ROIs. This imprecision likely reflects a combination of eye-tracker error and participants becoming aware that it was not necessary to precisely fixate the gaze cue dots to complete each trial. The lack of precision is plausible, given that requiring participants to make multiple eye movements within the relatively brief retention period essentially introduced a dual-task component to the delayed estimation tasks. The second eye movement (first peripheral gaze cue $>$ second peripheral gaze cue) was larger than the first eye movement (central fixation $>$ first peripheral gaze cue) in both conditions (BF $> 1{,}000$), so having to perform this larger movement under time pressure may explain why the error was larger in the second eye movement when compared with the first. Participants took longer to shift their gaze to the first gaze cue than the second gaze cue (BF $> 1{,}000$). This likely reflects the fact that the first gaze cue was presented in an unknown location, whereas the second gaze cue always appeared opposite the first, so participants were able to anticipate the second movement.

Experiment 2

Precision and guess rate are modulated by memory and eye-movements manipulations.

Similar to *E1*, location recall precision was high and guess rates were low (Fig. 9). The overall pattern of results was the same. Precision was reduced and guessing increased when participants were required to recall color compared with spatial location (BF Memory $> 1{,}000$). There was an interaction between the memory and eye-movements manipulations for precision (BF $> 1{,}000$), such that eye movements during retention caused a decline in location recall (BF $> 1{,}000$) but had no effect on color recall (BF < 1).

Alpha lateralization is modulated by eye movements and memory demands.

Alpha lateralization showed similar patterns of disruption in response to eye movements and memory demands as in *E1*. One-sample comparisons against zero were computed for lateralization indices in all conditions averaged across time

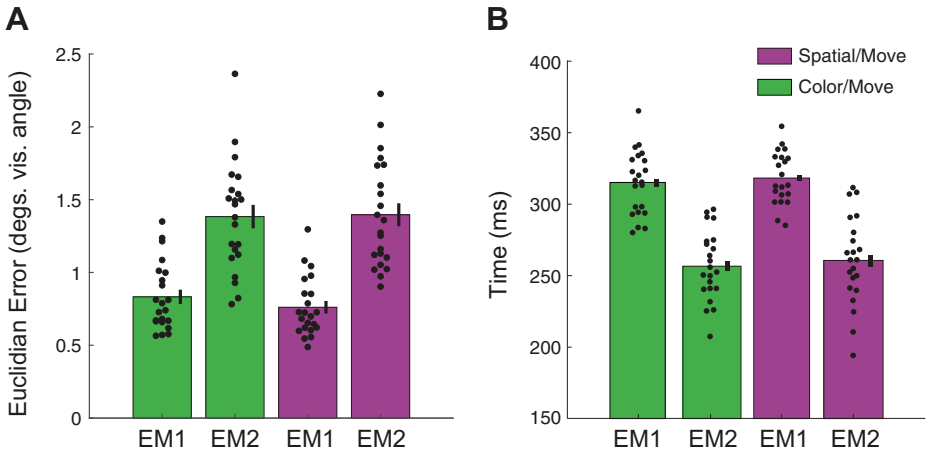

Figure 8. Eye-movements analysis (*experiment 1*). *A*: Euclidian error (minimum distance between eye-gaze cue and actual eye gaze) for the first and second eye-movements windows [eye-movements cue 1 (EM1) and eye-movements cue 2 (EM2), respectively] for both "move" conditions. *B*: time during each eye-movements window where actual eye gaze was closest to gaze cue. Error bars = means ±SE.

windows of interest. The tests revealed lateralization across all conditions during stimulus presentation (all BF >1,000; Fig. 10) and during the first eye-movements window (all BF > 30). However, in the return-to-fixation time window consistent lateralization was only observed in the fixation conditions (BF > 3) but not the move conditions (BF < 3).

Bayes factor ANOVAs computed to investigate lateralization differences between conditions within each time window revealed no differences in lateralization indices during stimulus presentation (all BFs < 1) suggesting that stimulus presentation had a consistent effect on alpha topography across all conditions. During the first eye-movements window, statistical models containing memory and eye-movements factors, as well as the interaction, had large Bayes factors (BF > 1,000), and follow-up pairwise comparisons confirmed reduced lateralization during both time windows in spatial/move when compared with spatial/fix (BF > 30) and color/move when compared with color/fix (BF >10). In the RF window, models containing memory and eye-movements factors as well as the interaction had large Bayes factors (BF > 10), and follow-up pairwise comparisons confirmed this was driven by differences in color/fix and color/move conditions (BF >3).

Together, these results confirm that shifts in posterior alpha were driven by stimulus presentation as expected, but alpha topography was only consistently lateralized throughout the entire retention period if participants were required to maintain spatial information and to not make eye movement.

Stored location-selective representations are degraded by eye movements.

Spatially selective CRFs were reconstructed from topographically specific patterns of total alpha power using the IEM technique. CRFs for each condition are shown in Fig. 11*A*. Real and permuted CRF slopes with statistical comparisons are shown in Fig. 11*B* and the actual Bayes factor results are shown in Fig. 11*C*. In Fig. 11*D*, the Bayes factor ANOVA models comparing the slopes of the real data across conditions are shown for all combinations of main and interaction effects and in Fig. 11*E* the follow-up Bayes factor pairwise comparisons.

Consistent with *E1*, CRF slopes increased in all conditions following stimulus onset (Fig. 11*B*) and peaked just after stimulus offset in all conditions except in color/fix, where it spiked again early in the retention period (~0.75 s). Slope was attenuated in response to the stimulus in conditions where participants were required to move their eyes during retention, and the decline during the early retention period was more rapid (see Fig. 11*D*, BF eyes and Fig. 11*E* from ~0.25 s onward). Again, the modulation of stimulus-related processing in the eye-movements conditions may suggest that anticipation of moving the eye during the forthcoming retention period causes location to be represented at lower fidelity.

Throughout the retention period, slope remained different from the permuted baseline in spatial/fix and color/fix conditions, except for the final 0.2 s of the color/fix condition.

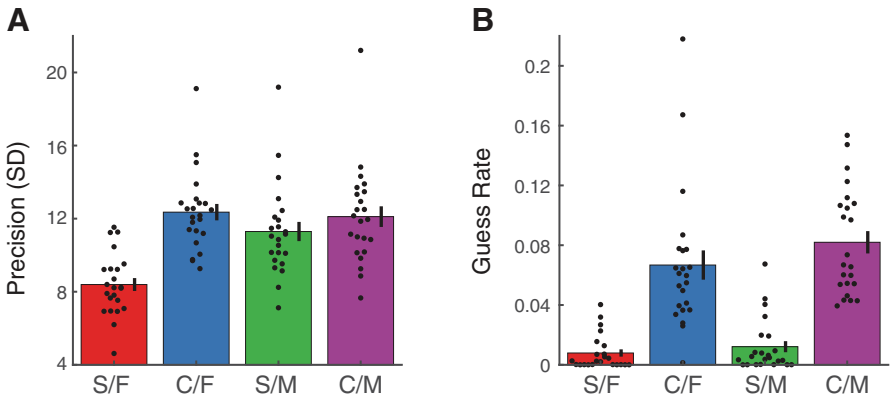

Figure 9. Behavior (*experiment 2*). Precision (SD in degrees from true location) (*A*) and guess rate (*B*, proportion of guess trials, i.e., where there was no memory) are shown for all conditions. In this and subsequent figures, the conditions are labeled as follows: S/F, Spatial/Fixate; C/F, Color/Fixate; S/M, Spatial/Move; C/M, Color/Move. Error bars = means ± SE.

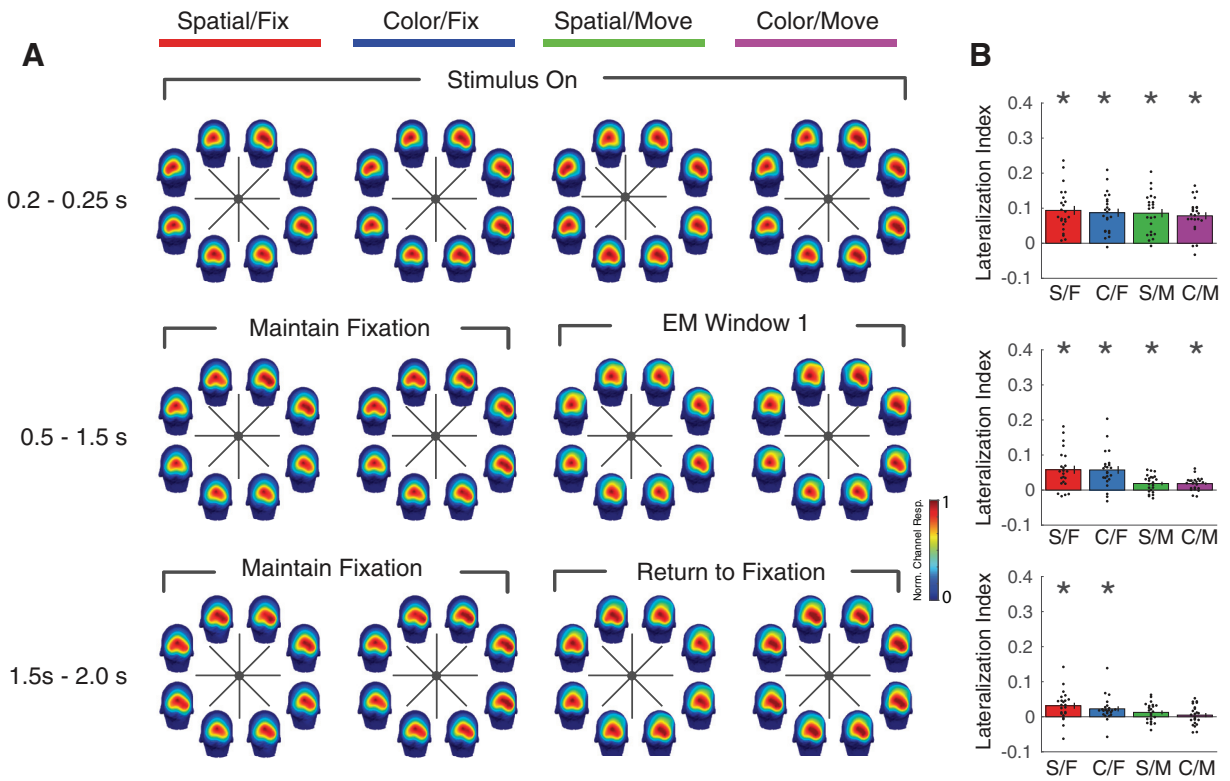

Figure 10. Alpha lateralization (*experiment 2*). *A*: topographic plots depict the distribution of alpha power across the scalp, averaged across trials and participants. Columns represent the four conditions. Rows represent the final 50 ms of stimulus presentation (0.2–0.25 s) and the retention period divided into the Eye-Movements Window 1 (0.5–1.5 s) and the Return to Fixation window (1.5–2.0 s). Note that the "fixate" conditions are divided into the same time windows so that alpha topography and lateralization can be compared between "fixate" and "move" conditions. The position of each head plot in the ring of plots reflects the mean activity across all trials where the stimulus was presented in the corresponding angular location bin. *B*: bar plots depict α lateralization indices for all conditions and time windows. Each row corresponds to the time window and topographic plots denoted in *A*. Higher values reflect greater lateralization. *Lateralization index significantly different to zero (Bayes factors, BF $>$ 3). S/F, Spatial/Fixate; C/F, Color/Fixate; S/M, Spatial/Move; C/M, Color/Move. Error bars = means ± SE.

Sustained slope throughout retention in the spatial/fix condition and the decline in slope around at the end of the color/fix condition are broadly consistent with *E1*, except here the representation does not re-emerge right at the very end of the color/fix condition. In both eye-movements conditions, slope initially declined at a similar rate. The spatial/move condition was no different from the permuted baseline from ~0.85 to 1.70 s, where the location representation re-emerged. The color/move condition was also not different from the baseline from ~0.90 s onward, except for when the representation very briefly re-emerged at ~1.37 s before falling back below the BF $<$ 3 threshold again for the remainder of retention.

Together with the data from *E1*, these data imply that eye movements disrupt the maintenance of spatial information coded in alpha, even when gaze is held stable in a new location during the retention period.

Generalization analyses reveal neural coding dynamics during eye-movements windows.

Temporal generalization analyses (21) computed for *E2* data revealed a very similar pattern of results to *E1* for the spatial/fix, spatial/move, and color/move conditions. Within the spatial/fix condition, there was consistent coding (Fig. 12, Spatial/Fix) along the diagonal and extensive generalization back and forward in time throughout stimulus presentation and retention. In both eye-movements conditions, there was no robust activation along the diagonal and no generalization beyond the first eye-movements window (0.5–1 s) in retention (Fig. 12, Spatial/Move and Color/Move), aside from what are likely carry-over effects from the stable gaze period before the first eye-movements cue. Together, these results suggest that spatial coding in alpha does not generalize when eye gaze is repositioned away from fixation after encoding and held stable for an extended duration. In the color/fix condition (Fig. 12, Color/Fix), there was robust encoding along the diagonal up until the decline at the end of retention, and good generalization back and forward in time throughout stimulus presentation and retention, with the exception of a few gaps. The generalization observed in this condition was more widespread than in the identical condition in E1 where generalization failure was observed later in the retention period (Fig. 6, Color/Fix).

Robust location-selective representations are not present outside the alpha-band during eye movements.

IEM analyses were computed from 1 to 30 Hz for both total and evoked power. The total power results were consistent with *E1*, such that spatial location was represented primarily in the alpha band (and some theta) during stimulus presentation in

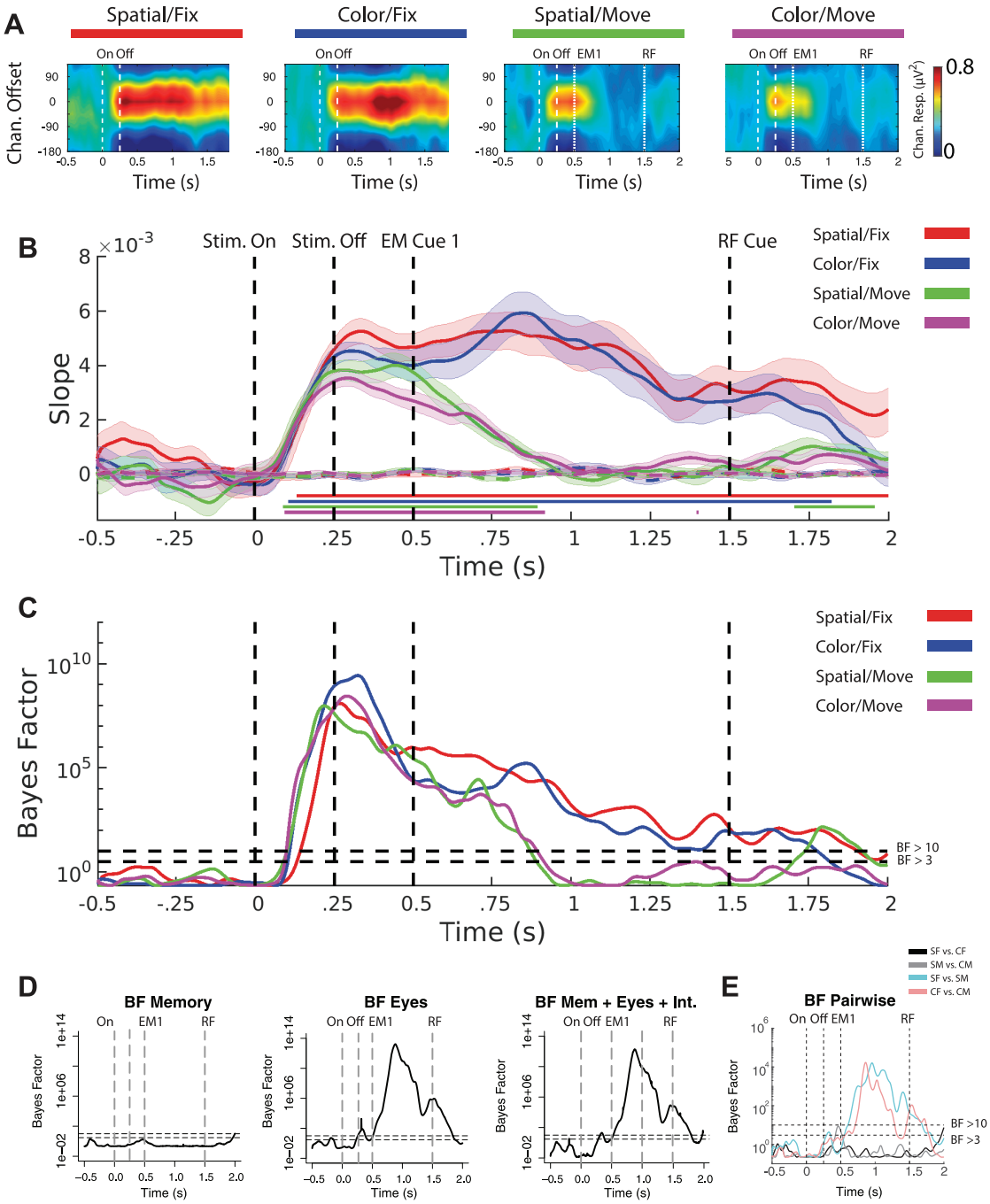

Figure 11. Modeling total alpha power (*experiment 2*). *A*: estimated channel response functions (CRFs) presented as heatmaps. *B*: CRF slopes, computed by folding each CRF at the peak channel offset at each time point and computing linear slope. Horizontal bars at base of plot indicate time points where there is moderate evidence for a statistical difference between each real CRF and its permuted baseline (Bayes factors, BF $>$ 3). *C*: actual BF values for tests comparing each real CRF and its permuted baseline. *D*: BF ANOVA model results comparing the "real" slope data across conditions (horizontal dashed lines indicate BF $>$ 3 and BF $>$ 10, respectively). *E*: BF pairwise comparisons comparing the "real" slope data (horizontal lower and upper dashed lines indicate BF $>$ 3 and BF $>$ 10, respectively). Dashed vertical lines in all plots indicate stimulus onset (On) and offset (Off) and the two eye-movements cues [eye-movements cue 1 (EM1) and return to fixation (RF)].

all conditions and then almost exclusively in alpha during retention in the "fixed" conditions but not consistently in alpha or any other bands during retention. The evoked power analyses were also consistent with *E1* such that location was represented in alpha and theta around the stimulus presentation time window. However, the key difference between these data and *E1* is that we do not observe persistent location coding in evoked theta throughout the entire retention period in the eye-movement conditions. One possible explanation for these different results is that the eye-movements schedule in *E2* was less taxing than in *E1*, meaning cognitive control demands were reduced and spatially selective activity in the lower frequency bands was not sufficient to be detected by the IEM (Fig. 13).

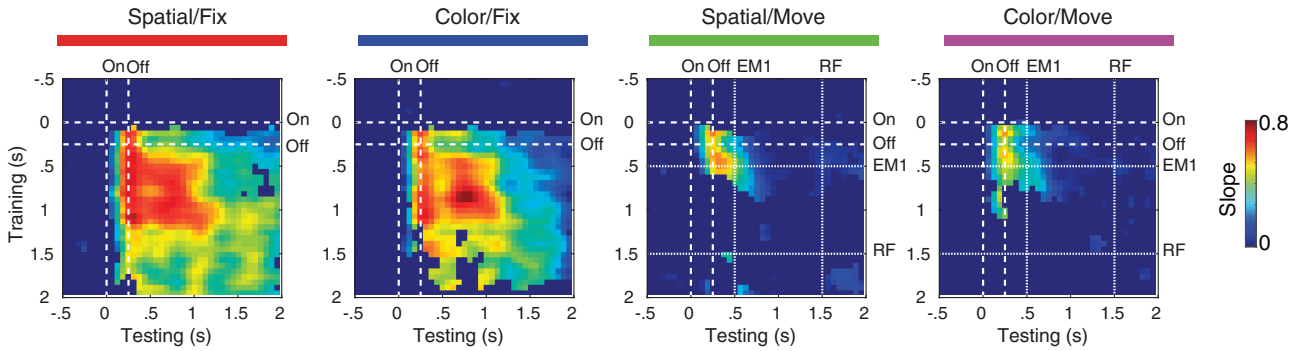

Figure 12. Temporal generalization of channel response functions (CRFs) (*experiment 2*). The linear slopes of the CRFs are plotted for each training and testing time-point, with greater slopes represented as hotter colors. Time-points where there is no statistical difference between real and permuted slope (Bayes factors, BF < 3) are plotted as uniform dark blue. Training and testing within each time-point [as per the previous inverted encoding modeling (IEM) analysis] is represented by activation along the diagonal stretching from the *top-left* to the *bottom-right* corners of each plot. Off-diagonal activations represent encoding endurance both backward in time (activations to the left of the diagonal) and forward in time (activations to the right of the diagonal). Dashed horizontal and vertical lines indicate stimulus onset (On) and offset (Off) and the two eye-movements cues [EM and return to fixation (RF)].

Eye movements.

The goal of *E2* was to determine whether it was possible to reconstruct CRFs when the eye gaze was repositioned away from fixation during the retention period and held stable at this new location before being returned to fixation. Gaze-contingent tracking ensured that participants moved their eyes as instructed, but as in *E1* it was necessary to set a fairly liberal ROI (1.6° visual angle radius) around the cue to allow for discrepancies between the actual gaze position and the position detected by the eye-tracker. To determine the size of the error between the eye position according to the tracker and the actual position of the eye movements cue, we computed the Euclidian distance between the eye position and cue over the course of each trial and then averaged across trials and participants (Fig. 14). The data indicate that when gaze had moved to the newly cued location and stabilized (~750 ms) the average error was ~1° visual angle in both conditions.

GENERAL DISCUSSION

Previous research has demonstrated that patterns of oscillatory activity in the alpha band play an important role in supporting the maintenance of spatial information (6, 7) and these ongoing representations are selectively modulated, but not abolished, by different forms of interruption to visual input (2, 5). The first goal of the present study was to determine whether changes to the retinotopic map that occur with eye movements would similarly affect spatial representations in alpha, or whether such a change abolishes the representation in alpha. The latter suggesting, in the presence of successful memory encoding and retention, that spatial WM is not entirely dependent on alpha as a mechanism for maintaining a representation of spatial location. The second goal was to determine whether alpha oscillations support coding of item location during disruptions of continuous visual input by eye movements even when location is not the to-be-remembered feature. Exploratory analyses were also carried out on frequency bands outside of alpha to explore alternative mechanisms for the representation of location in WM during eye movements.

Across two experiments, separate groups of participants completed trials of a delayed spatial estimation task, where they encoded and recalled the location or color of a probe after a brief retention period, and either maintained fixation or made a sequence of guided eye movements during retention. In *E1* participants made three eye movements, with the intention of disrupting patterns of alpha during the retention period; whereas in *E2* they only made two eye movements, with the goal being to preserve an extended time window (~1 s) where eye gaze was stable but allocated away from fixation and where the original spatial stimulus had been encoded. In both experiments, alpha lateralization analyses confirmed that eye movement changed the distribution of alpha across the scalp, reducing lateralization at a gross level. Furthermore, the primary IEM analyses revealed that while spatially specific representations could be reliably recovered from total alpha power during and immediately after stimulus encoding, these representations were only maintained throughout the entire retention period if the location was task-relevant and gaze fixed at the center i.e., not during eye movements. However, exploratory IEM analyses indicated that the retained item location information can be represented in lower frequency bands but only when participants were required to execute a demanding, rapid sequence of guided eye movements during the retention period.

Behaviorally, requiring participants to move their eyes during the retention period did result in reduced spatial precision in both experiments, which is broadly consistent with the degraded spatial representations observed in the brain data. One potential explanation is that the decline in precision due to eye movements reflects a change in memorization strategy, such that the spatial location of the probe shifts from being represented as a visual memory to a verbal memory, e.g., the probe appeared "North-West" relative to fixation. Guess rate did not increase as a function of eye movements, which could be interpreted as no reduction of the presence of the memory trace, or perhaps that the memory trace has successfully shifted from visual to another modality. However, recent arguments suggest that drawing a theoretical distinction between guess rate and precision effects from mixture models and interpreting them independently is problematic (53) so

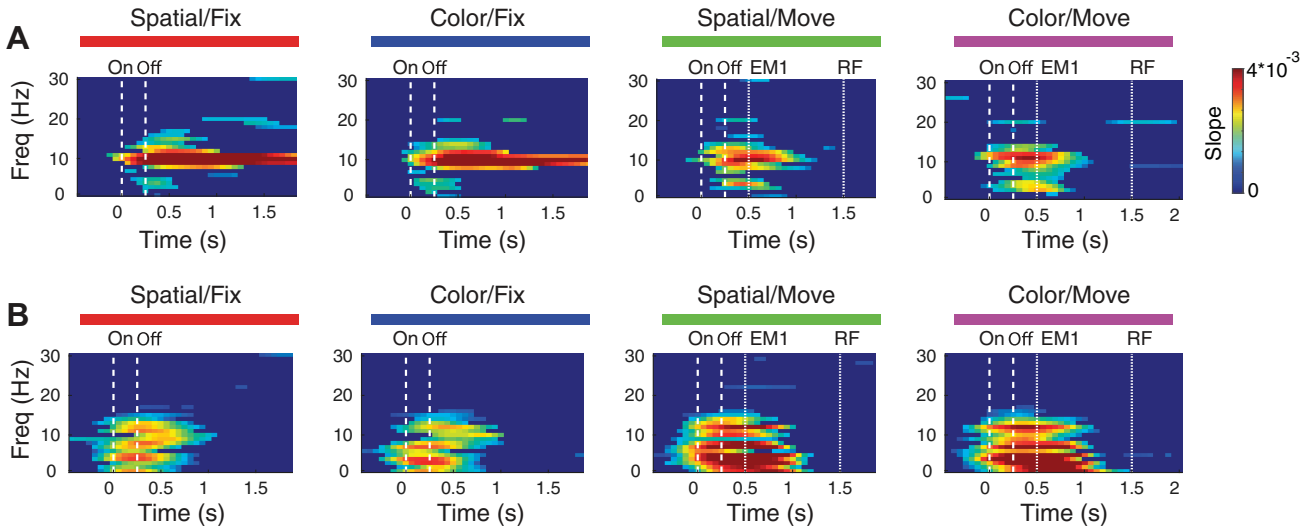

Figure 13. Tracking location-selective representations across a broad range of frequency bands for total (*A*) and evoked power (*experiment 2*) (*B*). Channel response functions (CRFs) slopes are plotted for each time sample across frequency bands 1–30 Hz. For each sample, the slope of the real CRF is compared with the permuted baseline and if the resulting Bayes factors (BF) < 3 then the point is represented in uniform dark blue. Dashed vertical lines indicate stimulus onset (On) and offset (Off) and the three eye-movements cues [eye-movements cue 1 (EM1), eye-movements cue 2 (EM2), and return to fixation (RF)].

our conclusion is that while precision declines as a function of eye movements, overall performance remains relatively intact.

Eye movements interrupt the continuous sampling of visual information by changing the mapping of the external environment onto the retina and disrupting the focus of overt spatial attention (12–15). Previous work demonstrated that the visual system's native representation of spatial attention is retinotopic, such that attention to a spatial location can linger in retinotopic coordinates for several hundred milliseconds after the execution of a saccade, and remapping to spatiotemporal (i.e., world-centered) coordinates occurs slowly and only if relevant to behavioral goals (16). Evidence from human neuroimaging indicates that when top-down signals work to remap and redirect spatial attention to new locations after eye movements, the retinotopic trace of a previously attended location persists throughout the visual cortex after a saccade (18); however, the role of alpha oscillations in the maintenance and remapping of items in visual memory after an eye movement was unknown. The present results confirm that spatial location representations in alpha are disrupted by eye movements; a result that is perhaps not surprising given that the disruptive effects of eye movements on the EEG signal are well documented. The extent of the disruption by eye movements was similar regardless of whether location or color was the to-be-remembered feature, although the representation did recover slightly earlier in the retention period immediately before location recall when compared to color recall. These results suggest that eye movements degrade stored location-selective representations in alpha in a way that is consistent with other forms of acute visual disruption, such as redirection of spatial attention, backward masking of the stimulus, or eye blinks (2, 5). The generalization analyses indicate that no distinct pattern of alpha emerged to support the maintenance of spatial information during the retention period, as is the case during extended eye closure (2). This outcome seems reasonable, given that in the present study, the eye-movements condition required the rapid redirection of both spatial attention and eye gaze several times during retention, so this has more in common with other forms of acute visual disruptions than extended eye closure, which is comparatively slow and presumably requires attention to be redirected toward an internalized representation of the location.

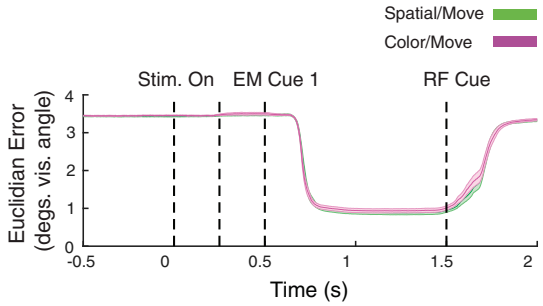

Figure 14. Eye-movements analysis (*experiment 2*). Euclidian error (minimum distance between eye-gaze cue and actual eye gaze) throughout the trial for both "move" conditions. Error bars = means ± SE. EM, eye movement; RF, return to fixation.

If eye movements disrupt the maintenance of spatially selective representations in alpha, then this raises the question of how and where the representations are stored, given that these representations must still exist in some form as participants are still able to recall object locations with a high level of accuracy in the eye-movements conditions. One explanation is that location is coded in alpha but stored in retinotopic coordinates that are updated with each saccade (17). Requiring participants to saccade to different locations during retention causes misalignment of the retinotopic coordinates, thus preventing reconstruction of the spatiotopic location. This may explain why spatial location cannot be reconstructed during the eye-movements phase of retention but can be reconstructed once the gaze has been returned to central fixation at the end of the trial. It is possible that location is

still represented in alpha, but we are simply unable to reconstruct it using the IEM approach.

An alternative (or perhaps complementary) explanation is that frequency bands outside of alpha may play a role in representing spatial information when eye gaze is redirected during the retention period. Here, exploratory analyses revealed consistent location coding in evoked theta throughout retention in the eye-movements conditions in *E1* but not *E2*. One potential explanation is that the lower frequency bands are recruited to help code for retained spatial information when the visual environment is destabilized by multiple eye movement and/or when task demands require increased cognitive control. Theta plays a role in irrelevant information suppression (54) and interruptions in a WM task can modulate nonlateralized theta power (55), so it is plausible that theta is also involved in helping retain spatial information during sequences of guided eye movements. Indeed, low-frequency oscillations in frontal cortex and frontal-parietal interactions are involved in executive control in WM tasks and one hypothesis is that frontal cortex controls switching between representational states in multitask sequences via these oscillations (26). Interestingly, theta represents retained item location information regardless of whether item location is the to-be-remembered feature, suggesting that the lower frequencies may be involved in coding for spatial information regardless of behavioral relevance. To our knowledge, the present study is the first IEM study in humans to demonstrate that lower frequency bands can be recruited to maintain location-selective representations in WM. However, these exploratory findings must be interpreted with caution as the effects are only statistically different from the permuted baseline during specific 1 Hz bands in the theta/delta range and are nowhere not as robust as the effects observed in alpha.

The primary goal of this study was to investigate the disruptive effects of eye movements on item location coding in alpha. However, the results from the color/fix condition provide interesting insight into how spontaneously coded spatial information is maintained in working memory, so they are also worthy of discussion. First, persistent spontaneous coding of spatial information in a task where spatial information is goal-irrelevant is consistent with previous results (7; *experiment 1*), although here we show that there is a limit to the duration of this spatial coding. Second, in both experiments the location-selective responses reconstructed from alpha-band activity in both fixation conditions initially peak just after stimulus onset in all conditions, but then in the color/fix condition they reach an even higher peak around 0.8 s whereas in the spatial/fix condition they stay relatively flat or decline. Given that probe location is not behaviorally relevant in the color/fix condition, this begs the question of why location coding is particularly robust during this time window in the retention period. One speculative explanation could be that this bump reflects the binding of spatial location and retained color in WM.

CONCLUSIONS

In summary, this study used an IEM approach to examine how stored spatial location representations in WM are modulated by eye movements. The findings indicate that retained spatial information in the alpha band is degraded by eye movement in a similar way to other acute visual interruptions such as shifts of visuospatial attention, backward masking of the stimulus, and eye blinks. However, the results also suggest that under certain task conditions, frequency bands outside alpha can be recruited to maintain spatial information whereas the eye movements are ongoing, which may go some way toward explaining why spatial WM performance remained relatively intact despite eye movements. Furthermore, the data show that spontaneously encoded spatial information in alpha is maintained for a limited duration and possibly supported by dual coding processes. This work helps clarify how mental representations in visuospatial WM are modulated by visual disruptions and opens the door for further investigations of eye movements effects on WM.

DATA AVAILABILITY

All custom scripts and anonymized data are available at https://github.com/attlab/Eye_Movements_Disrupt_Alpha_WM.

ACKNOWLEDGMENTS

We thank our undergraduate research assistants Dana Shevachman and Kayla Chambers for assistance with data collection.

GRANTS

This work was generously supported by the Institute for Collaborative Biotechnologies through cooperative Agreement W911NF-19-2-0026 from the U.S. Army Research Office. The content of the information does not necessarily reflect the position or the policy of the Government and no official endorsement should be inferred. This work was also supported by Undegraduate Research and Creative Activities (URCA) Grants (to K. Pickett and A. Salimian) provided by the University of California, Santa Barbara.

DISCLOSURES

No conflicts of interest, financial or otherwise, are declared by the authors.

AUTHOR CONTRIBUTIONS

T.B., K.P., A.S., M.H.M., and B.G. conceived and designed research; T.B., K.P., A.S., C.G., and M.H.M. performed experiments; T.B., K.P., A.S., C.G., M.H.M., and B.G. analyzed data; T.B., K.P., A.S., M.H.M., and B.G. interpreted results of experiments; T.B., K.P., and A.S. prepared figures; T.B., K.P., A.S., C.G., M.H.M., and B.G. drafted manuscript; T.B., K.P., A.S., C.G., M.H.M., and B.G. edited and revised manuscript; T.B., K.P., A.S., C.G., M.H.M., and B.G. approved final version of manuscript.

REFERENCES

1. **Garrett J**, **Bullock T**, **Giesbrecht B.** Tracking the contents of spatial working memory during an acute bout of aerobic exercise. *J Cogn Neurosci* 33: 1271–1286, 2021. doi:10.1162/jocn_a_01714.
2. **MacLean MH**, **Bullock T**, **Giesbrecht B.** Dual process coding of recalled locations in human oscillatory brain activity. *J Neurosci* 39: 6737–6750, 2019. doi:10.1523/JNEUROSCI.0059-19.2019.
3. **Samaha J**, **Sprague TC**, **Postle BR.** Decoding and reconstructing the focus of spatial attention from the topography of alpha-band oscillations. *J Cogn Neurosci* 28: 1090–1097, 2016. doi:10.1162/jocn_a_00955.
4. **Thut G**, **Nietzel A**, **Brandt SA**, **Pascual-Leone A.** Alpha-band electroencephalographic activity over occipital cortex indexes visuospatial

attention bias and predicts visual target detection. *J Neurosci* 26: 9494–9502, 2006. doi:10.1523/JNEUROSCI.0875-06.2006.
5. **van Moorselaar D**, **Foster JJ**, **Sutterer DW**, **Theeuwes J**, **Olivers CNL**, **Awh E.** Spatially selective alpha oscillations reveal moment-by-moment trade-offs between working memory and attention. *J Cogn Neurosci* 30: 256–266, 2018. doi:10.1162/jocn_a_01198.
6. **Foster JJ**, **Sutterer DW**, **Serences JT**, **Vogel EK**, **Awh E.** The topography of alpha-band activity tracks the content of spatial working memory. *J Neurophysiol* 115: 168–177, 2016. doi:10.1152/jn.00860.2015.
7. **Foster JJ**, **Bsales EM**, **Jaffe RJ**, **Awh E.** Alpha-band activity reveals spontaneous representations of spatial position in visual working memory. *Curr Biol* 27: 3216–3223.e6, 2017. doi:10.1016/j.cub.2017.09.031.
8. **Dill M**, **Fahle M.** Limited translation invariance of human visual pattern recognition. *Percept Psychophys* 60: 65–81, 1998. doi:10.3758/BF03211918.
9. **Rajsic J**, **Wilson DE.** Asymmetrical access to color and location in visual working memory. *Attent Percept Psychophys* 76: 1902–1913, 2014. doi:10.3758/s13414-014-0723-2.
10. **Schneegans S**, **Bays PM.** Neural architecture for feature binding in visual working memory. *J Neurosci* 37: 3913–3925, 2017. doi:10.1523/JNEUROSCI.3493-16.2017.
11. **Theeuwes J**, **Kramer AF**, **Irwin DE.** Attention on our mind: the role of spatial attention in visual working memory. *Acta Psychol* 137: 248–251, 2011. doi:10.1016/j.actpsy.2010.06.011.
12. **Irwin DE.** Integrating information across saccadic eye movements. *Curr Direct Psychol Sci* 5: 94–100, 1996. doi:10.1111/1467-8721.ep10772833.
13. **Kowler E**, **Anderson E**, **Dosher B**, **Blaser E.** The role of attention in the programming of saccades. *Vision Res* 35: 1897–1916, 1995. doi:10.1016/0042-6989(94)00279-U.
14. **McPeek RM**, **Maljkovic V**, **Nakayama K.** Saccades require focal attention and are facilitated by a short-term memory system. *Vision Res* 39: 1555–1566, 1999. doi:10.1016/S0042-6989(98)00228-4.
15. **Rolfs M**, **Jonikaitis D**, **Deubel H**, **Cavanagh P.** Predictive remapping of attention across eye movements. *Nat Neurosci* 14: 252–258, 2011. doi:10.1038/nn.2711.
16. **Golomb JD**, **Chun MM**, **Mazer JA.** The native coordinate system of spatial attention is retinotopic. *J Neurosci* 28: 10654–10662, 2008. doi:10.1523/JNEUROSCI.2525-08.2008.
17. **Golomb JD**, **Kanwisher N.** Retinotopic memory is more precise than spatiotopic memory. *Proc Natl Acad Sci USA* 109: 1796–1801, 2012. doi:10.1073/pnas.1113168109.
18. **Golomb JD**, **Nguyen-Phuc AY**, **Mazer JA**, **McCarthy G**, **Chun MM.** Attentional facilitation throughout human visual cortex lingers in retinotopic coordinates after eye movements. *J Neurosci* 30: 10493–10506, 2010. doi:10.1523/JNEUROSCI.1546-10.2010.
19. **Jensen O**, **Pan Y**, **Frisson S**, **Wang L.** An oscillatory pipelining mechanism supporting previewing during visual exploration and reading. *Trends Cogn Sci* 25: 1033–1044, 2021. doi:10.1016/j.tics.2021.08.008.
20. **Garcia JO**, **Srinivasan R**, **Serences JT.** Near-real-time feature-selective modulations in human cortex. *Curr Biol* 23: 515–522, 2013. doi:10.1016/j.cub.2013.02.013.
21. **King J**, **Dehaene S.** Characterizing the dynamics of mental representations: the temporal generalization method. *Trends Cogn Sci* 18: 203–210, 2014. doi:10.1016/j.tics.2014.01.002.
22. **Foster JJ**, **Sutterer DW**, **Serences JT**, **Vogel EK**, **Awh E.** Alpha–band oscillations enable spatially and temporally resolved tracking of covert spatial attention. *Psychol Sci* 28: 929–941, 2017. doi:10.1177/0956797617699167.
23. **Cavanagh JF**, **Frank MJ.** Frontal theta as a mechanism for cognitive control. *Trends Cogn Sci* 18: 414–421, 2014. doi:10.1016/j.tics.2014.04.012.
24. **Lisman J.** Working memory: the importance of theta and gamma oscillations. *Curr Biol* 20: R490–R492, 2010. doi:10.1016/j.cub.2010.04.011.
25. **Sauseng P**, **Griesmayr B**, **Freunberger R**, **Klimesch W.** Control mechanisms in working memory: a possible function of EEG theta oscillations. *Neurosci Biobehav Rev* 34: 1015–1022, 2010. doi:10.1016/j.neubiorev.2009.12.006.
26. **de Vries IEJ**, **Slagter HA**, **Olivers CNL.** Oscillatory control over representational states in working memory. *Trends Cogn Sci* 24: 150–162, 2020. doi:10.1016/j.tics.2019.11.006.
27. **Brainard DH.** The psychophysics toolbox. *Spat Vis* 10: 433–436, 1997. doi:10.1163/156856897X00357.
28. **Suchow JW**, **Brady TF**, **Fougnie D**, **Alvarez GA.** Modeling visual working memory with the MemToolbox. *J Vis* 13: 9, 2013. doi:10.1167/13.10.9.
29. **Delorme A**, **Makeig S.** EEGLAB: an open source toolbox for analysis of single-trial EEG dynamics including independent component analysis. *J Neurosci Methods* 134: 9–21, 2004. doi:10.1016/j.jneumeth.2003.10.009.
30. **Gomez-Herrero G**, **Clercq W**, **Anwar H**, **Kara O**, **Egiazarian K**, **Huffel S**, **Paesschen W.** Automatic removal of ocular artifacts in the EEG without an EOG reference channel. In: *Proceedings of the 7th Nordic Signal Processing Symposium—NORSIG 2006*. New York: IEEE, 2006, p. 130–133. doi:10.1109/NORSIG.2006.275210.
31. **Kelly SP**, **Lalor EC**, **Reilly RB**, **Foxe JJ.** Increases in alpha oscillatory power reflect an active retinotopic mechanism for distracter suppression during sustained visuospatial attention. *J Neurophysiol* 95: 3844–3851, 2006. doi:10.1152/jn.01234.2005.
32. **Sauseng P**, **Klimesch W**, **Stadler W**, **Schabus M**, **Doppelmayr M**, **Hanslmayr S**, **Gruber WR**, **Birbaumer N.** A shift of visual spatial attention is selectively associated with human EEG alpha activity. *Eur J Neurosci* 22: 2917–2926, 2005. doi:10.1111/j.1460-9568.2005.04482.x.
33. **Sprague TC**, **Adam KCS**, **Foster JJ**, **Rahmati M**, **Sutterer DW**, **Vo VA.** Inverted encoding models assay population-level stimulus representations, not single-unit neural tuning. *eNeuro* 5: ENEURO.0098-18.2018, 2018. doi:10.1523/ENEURO.0098-18.2018.
34. **Gardner JL**, **Liu T.** Inverted encoding models reconstruct an arbitrary model response, not the stimulus. *eNeuro* 6: ENEURO.0363-18.2019, 2019. doi:10.1523/ENEURO.0363-18.2019.
35. **Liu T**, **Cable D**, **Gardner JL.** Inverted encoding models of human population response conflate noise and neural tuning width. *J Neurosci* 38: 398–408, 2017. doi:10.1523/JNEUROSCI.2453-17.2017.
36. **Sprague TC**, **Boynton GM**, **Serences JT.** The importance of considering model choices when interpreting results in computational neuroimaging. *ENeuro* 6: ENEURO.0196-19, 2019. doi:10.1523/ENEURO.0196-19.2019.
37. **Ito J**, **Maldonado P**, **Singer W**, **Grün S.** Saccade-related modulations of neuronal excitability support synchrony of visually elicited spikes. *Cerebral Cortex* 21: 2482–2497, 2011. 10.1093/cercor/bhr020.
38. **Katz CN**, **Patel K**, **Talakoub O**, **Groppe D**, **Hoffman K**, **Valiante TA.** Differential generation of saccade, fixation, and image-onset event-related potentials in the human mesial temporal lobe. *Cereb Cortex* 30: 5502–5516, 2020. doi:10.1093/cercor/bhaa132.
39. **Leszczynski M**, **Schroeder CE.** The role of neuronal oscillations in visual active sensing. *Front Integr Neurosci* 13: 32, 2019. doi:10.3389/fnint.2019.00032.
40. **Rajkai C**, **Lakatos P**, **Chen CM**, **Pincze Z**, **Karmos G**, **Schroeder CE.** Transient cortical excitation at the onset of visual fixation. *Cereb Cortex* 18: 200–209, 2008. doi:10.1093/cercor/bhm046.
41. **Kass RE**, **Raftery AE.** Bayes factors. *J Am Stat Assoc* 90: 773–795, 1995. doi:10.1080/01621459.1995.10476572.
42. **Kruschke JK**, **Liddell TM.** The Bayesian new statistics: hypothesis testing, estimation, meta-analysis, and power analysis from a Bayesian perspective. *Psychon Bull Rev* 25: 178–206, 2018. doi:10.3758/s13423-016-1221-4.
43. **Rouder JN**, **Morey RD**, **Speckman PL**, **Province JM.** Default Bayes factors for ANOVA designs. *J Math Psychol* 56: 356–374, 2012. doi:10.1016/j.jmp.2012.08.001.
44. **Morey RD**, **Rouder JN**, **Jamil T.** Package "Bayes Factor" (Online). http://www.icesi.edu.co/CRAN/web/packages/BayesFactor/BayesFactor.pdf [2018 May 19].
45. **Dienes Z.** How Bayes factors change scientific practice. *J Math Psychol* 72: 78–89, 2016. doi:10.1016/j.jmp.2015.10.003.
46. **Wetzels R**, **Matzke D**, **Lee MD**, **Rouder JN**, **Iverson GJ**, **Wagenmakers E-J.** Statistical evidence in experimental psychology. *Perspect Psychol Sci* 6: 291–298, 2011. doi:10.1177/1745691611406923.
47. **Gelman A**, **Tuerlinckx F.** Type S error rates classical and Bayesian single and multiple compparison procedures. *Comput Stat* 15: 373–390, 2000. doi:10.1007/s001800000040.
48. **Worden MS**, **Foxe JJ**, **Wang N**, **Simpson GV.** Anticipatory biasing of visuospatial attention indexed by retinotopically specific alpha-band electroencephalography increases over occipital cortex. *J Neurosci* 20: RC63, 2000. doi:10.1523/JNEUROSCI.20-06-j0002.2000.
49. **Di Russo F**, **Martínez A**, **Hillyard SA.** Source analysis of event-related cortical activity during visuo-spatial attention. *Cereb Cortex* 13: 486–499, 2003. doi:10.1093/cercor/13.5.486.

50. **Harter MR**, **Miller SL**, **Price NJ**, **LaLonde ME**, **Keyes AL.** Neural processes involved in directing attention. *J Cogn Neurosci* 1: 223–237, 1989. doi:10.1162/jocn.1989.1.3.223.
51. **Hopf JM**, **Mangun GR.** Shifting visual attention in space: an electrophysiological analysis using high spatial resolution mapping. *Clin Neurophysiol* 111: 1241–1257, 2000. doi:10.1016/S1388-2457(00)00313-8.
52. **Martínez A**, **Anllo-Vento L**, **Sereno MI**, **Frank LR**, **Buxton RB**, **Dubowitz DJ**, **Wong EC**, **Hinrichs H**, **Heinze HJ**, **Hillyard SA.** Involvement of striate and extrastriate visual cortical areas in spatial attention. *Nat Neurosci* 2: 364–369, 1999. doi:10.1038/7274.
53. **Schurgin MW**, **Wixted JT**, **Brady TF.** Psychophysical scaling reveals a unified theory of visual memory strength. *Nat Hum Behav* 4: 1156–1172, 2020. doi:10.1038/s41562-020-00938-0.
54. **Green JJ**, **McDonald JJ.** Electrical neuroimaging reveals timing of attentional control activity in human brain. *PLoS Biol* 6: 730–738, 2008. doi:10.1371/journal.pbio.0060081.
55. **Zickerick B**, **Rösner M**, **Sabo M**, **Schneider D.** How to refocus attention on working memory representations following interruptions—evidence from frontal theta and posterior alpha oscillations. *Eur J Neurosci* 54: 7820–7838, 2021. doi:10.1111/ejn.15506.